[U-^{14}C]-glucose (0.25 μCi mL^{-1}) and then incubated with tetrandrine at the desired concentrations at 37 °C for 1 h, the optimal time obtained from preliminary experiments, under continuous shaking. The incorporation of [U-^{14}C]-glucose into glycogen was determined by ethanol precipitation. The incorporation into glycogen was expressed as nanomoles per milligram of cell protein in 1 h or as the percentage of basal level that was obtained from hepatocytes incubated with KRBB only. Protein content was determined using the BioRad protein dye-binding assay.

Statistical analysis

Data are expressed as the mean ± s.e.m. for the number (n) of animals in the group, as indicated in the figures. Repeated measures of analysis of variance (ANOVA) were used to analyse the changes in plasma glucose and other parameters. The Dunnett range post-hoc comparisons were used to determine the source of significant differences where appropriate. The concentration that produced 50% of the maximum effect (EC_{50}) was obtained from nonliner regression analysis. A P value < 0.05 was considered statistically significant.

Results

Effects of tetrandrine on plasma glucose concentration in STZ-diabetic rats

Figure 2 shows a dose-dependent decrease of plasma glucose in STZ-diabetic rats that received treatment with tetrandrine; the maximal effect (24.2 ± 1.8%) was achieved with 1.0 mg kg^{-1} of tetrandrine. Increasing the tetrandrine dose to 1.5 mg kg^{-1} resulted in no further decrease in plasma glucose. Thus, 1.0 mg kg^{-1} of tetrandrine was employed in subsequent experiments.

However, the plasma glucose level in normal rats was not modified at 30 min after an i.v. injection of tetrandrine at the dose that was effective in STZ-diabetic rats. The plasma glucose level in normal rats was reduced by 35 min after the injection of tetrandrine. As shown in Figure 2, tetrandrine lowered the plasma glucose in normal rats by about 8.2 ± 1.0, 13.6 ± 1.4 and 18.3 ± 1.7% after dosing with 0.1, 0.5 and 1.0 mg kg^{-1}, respectively.

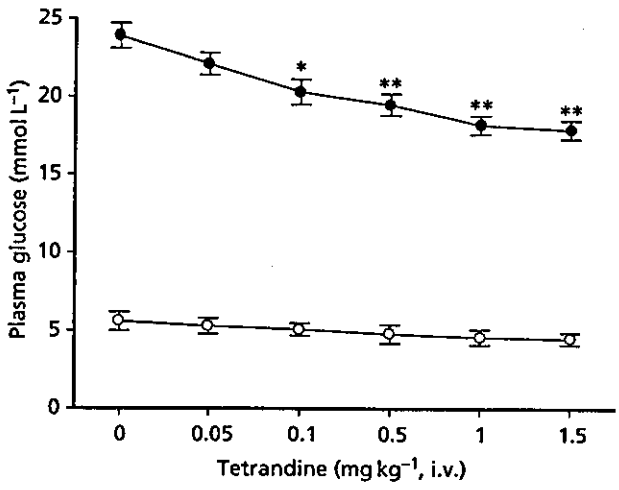

Figure 2 The plasma glucose lowering activity produced by an intravenous injection of tetrandrine into normal Wistar rats ○ and STZ-diabetic rats ●. Values (means ± s.e.m.) were obtained from each group of eight animals. Vehicle (0.9% NaCl in distilled water) was given at the same volume. *P < 0.05 and **P < 0.01 vs data from animals treated with vehicle (0).

Effects of tetrandrine on mean arterial blood pressure in STZ-diabetic rats

The effect of tetrandrine on mean arterial blood pressure at a dose (1.0 mg kg^{-1}) sufficient to lower plasma glucose was investigated. After injection of STZ for 1 week, the mean arterial blood pressure in diabetic rats was elevated to 128.5 ± 2.2 mmHg in a way markedly different (P < 0.05) to that in vehicle-treated control rats (105.4 ± 3.1 mmHg; n = 8). However, the mean arterial blood pressure in diabetic rats was not influenced (P > 0.05) by an i.v. injection of 1.0 mg kg^{-1} tetrandrine for 30 min (125.6 ± 2.8 mmHg; n = 8).

Effect of tetrandrine on the IVGCT

The effect of tetrandrine on the response of normal Wistar rats to the IVGCT is showed in Figure 3. The basal plasma glucose concentration in Wistar rats was 5.3 ± 0.5 mmol L^{-1}. Thirty minutes after i.v. treatment with tetrandrine (1.0 mg kg^{-1}), the plasma glucose level

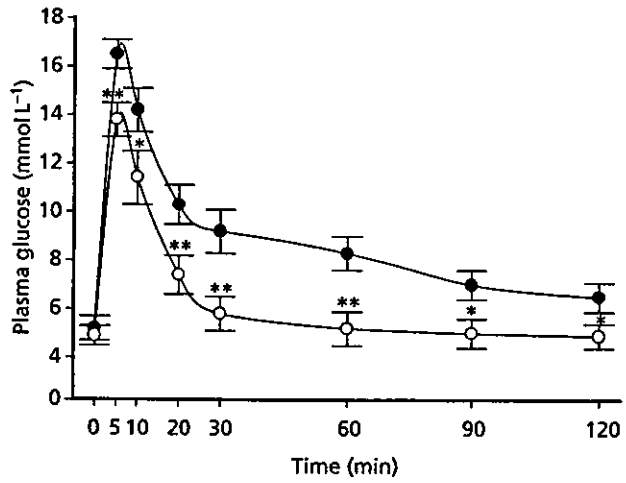

Figure 3 Effect of tetrandrine on plasma glucose concentration in normal rats receiving an IVGCT. Tetrandrine (1.0 mg kg^{-1}) was injected into the tail vein (○) and compared with the control group of rats receiving a similar injection of vehicle (0.9% NaCl in distilled water) at the same volume (●). The IVGCT was performed with an intravenous injection of glucose at 60.0 mg kg^{-1} into the two groups of rats 30 min later and the plasma glucose in samples obtained immediately was indicated as 0 min. Values (means ± s.e.m.) were obtained from eight rats in each group. *P < 0.05 and **P < 0.01 vs data from control group.

in rats was 4.9 ± 0.4 mmol L^{-1} in rats compared with 5.2 ± 0.5 mmol L^{-1} in vehicle-treated rats; these values were not significantly ($P > 0.05$) different from the basal level. Five minutes after the IVGCT, the plasma glucose concentration was elevated to 16.5 ± 0.6 mmol L^{-1} in vehicle-treated rats but was 13.8 ± 0.7 mmol L^{-1} in tetrandrine-treated rats. Tetrandrine at 1.0 mg kg^{-1} significantly attenuated the increase of plasma glucose following the IVGCT and the plasma glucose lowering activity was obtained 5 min after the IVGCT. The plasma glucose concentration in the tetrandrine-treated group undergoing the IVGCT was decreased almost to the basal level for the 30-min observation period.

Effect of tetrandrine on glucose uptake into soleus muscle

The time course of the stimulatory effect of tetrandrine on glucose uptake into soleus muscle was preliminarily determined. Glucose uptake was enhanced within 5 min of exposure to tetrandrine at 1.0 μmol L^{-1}. This action of tetrandrine was increased gradually. The longer incubation time achieved half-maximal stimulation at 10 min and maximal stimulation at 30 min, which was the optimal time used in the experiments. Stimulation of [^{14}C]-2-DG uptake by soleus muscle after a 30-min exposure of 1 nmol L^{-1} bovine insulin was about $212.5 \pm 4.5\%$ of the basal [^{14}C]-2-DG uptake (732.2 ± 20.2 pmol 5 min^{-1}) that was taken as 100% from samples incubated with KRBB only ($n = 6$). Tetrandrine increased the [^{14}C]-2-DG uptake into soleus muscle in a concentration-dependent manner (Figure 4). The EC_{50} of tetrandrine required to increase [^{14}C]-2-DG uptake into soleus muscle was about 0.1 μmol L^{-1}. Maximal [^{14}C]-2-DG uptake obtained in samples treated with tetrandrine at 1.0 μmol L^{-1} was 1319.4 ± 44.2 pmol 5 min^{-1}, which was about $180.2 \pm 5.7\%$ of the basal uptake although the activity was about 85% of that induced by bovine insulin at 1 nmol L^{-1}. The stimulatory effect of tetrandrine at 10.0 μmol L^{-1} was 1345.5 ± 52.4 pmol 5 min^{-1}, which is similar to the value obtained from 1.0 μmol L^{-1} of tetrandrine.

Effect of tetrandrine on glycogen synthesis in hepatocytes

In hepatocytes of STZ-diabetic rats, a 30-min exposure of 1 nmol L^{-1} bovine insulin increased the level of [^{14}C]-glucose incorporation into glycogen (3.6 ± 0.4 nmol mg^{-1} protein 1 h^{-1}) to about 2.4-fold of the basal glycogen synthesis (1.5 ± 0.3 nmol mg^{-1} protein 1 h^{-1}) that was taken as 100% from samples treated with same volume of KRBB ($n = 6$). Incubation with tetrandrine increased glycogen synthesis into the hepatocytes of STZ-diabetic rats significantly ($P < 0.05$) in a concentration-dependent manner, although the activity was less than that of bovine insulin (Figure 5). Tetrandrine at 1.0 μmol L^{-1} increased the glycogen synthesis in hepatocytes of STZ-diabetic rats to 2.5 ± 0.2 nmol mg^{-1} protein 1 h^{-1}, which was about 1.7 times the basal level. Even at 10 μmol L^{-1}, the higher concentration used, tetrandrine did not increase [^{14}C]-glucose incorporation into glycogen more markedly. The maximal activity of 1.0 μmol L^{-1} tetrandrine was about 75% of that induced by bovine insulin at 1 nmol L^{-1}. Similar to the effect on glucose uptake, the EC_{50} of tetrandrine on glycogen synthesis was about 0.1 μmol L^{-1}.

Discussion

In the present study we found that tetrandrine can lower the plasma glucose level in STZ-diabetic rats, an experimental model for type 1-like diabetes mellitus. Tetrandrine can also

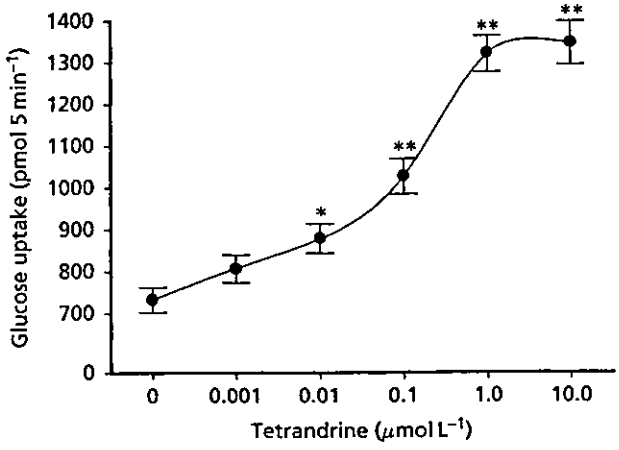

Figure 4 Effect of tetrandrine on the glucose uptake into soleus muscle isolated from STZ-diabetic rats. Values (mean ± s.e.m.) were obtained from each group of 10 animals. *$P < 0.05$ and **$P < 0.01$ vs data from samples incubated only with KRBB (0), respectively.

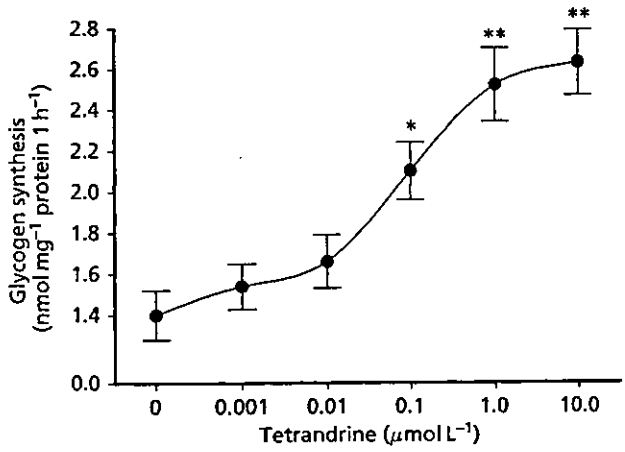

Figure 5 Effect of tetrandrine on the glucose incorporation into glycogen in hepatocytes isolated from STZ-diabetic rats. Values (mean ± s.e.m.) were obtained from each group of 10 animals. *$P < 0.05$ and **$P < 0.01$ vs data from samples incubated with only KRBB (0), respectively.

lower the plasma glucose level in normal rats but the onset time was slower (35 min) than in diabetic rats. The difference of onset time for intravenous injection of tetrandrine was only 5 min between diabetic and normal rats. It seems that the pharmacokinetic parameters for tetrandrine are similar between the two kinds of animals. However, the real mechanisms remain obscure and require further investigation.

Usually, diabetes mellitus is associated with hypertension (Cerielo et al 1997). Some hypoglycaemic agents, such as metformin and troglitazone, showed hypotensive effects in the animal model of diabetes (Kosegawa et al 1999). It has been documented that tetrandrine at a dose of 15.0 mg kg^{-1} acts as a calcium entry blocker to effectively lower blood pressure (Felix et al 1992) and mean arterial pressure (Hu et al 1987). Thus, the blood pressure measurement was performed to identify whether the plasma glucose lowering action of tetrandrine is linked to the reduction in blood pressure. In the present study, treatment with tetrandrine at doses sufficient to lower plasma glucose concentration failed to modify the mean arterial pressures in STZ-diabetic rats. The effective dose of tetrandrine for lowering of plasma glucose was less than that required for a decrease in blood pressure. The plasma glucose lowering effect of tetrandrine in STZ-diabetic rats therefore seems not to be related to the change in blood pressure.

Several methods have been established to assess glucose utilization and/or insulin sensitivity in animals and humans (Bessesen 2001). Using the IVGCT, we observed that tetrandrine (1.0 mg kg^{-1}) significantly attenuated the increase in plasma glucose following the IVGCT in Wistar rats when compared with the vehicle-treated group. Thus, enhancing glucose utilization can be considered for the plasma glucose lowering action of tetrandrine in vivo.

In diabetes, elevation of blood glucose is a consequence of increased hepatic glucose output together with reduced peripheral glucose utilization (Consoli et al 1989). Skeletal muscle is a major site for glucose disposal (Baron et al 1988). Glucose transportation, which depends on insulin-stimulated translocation of glucose carriers to the cell membrane, is the rate-limiting step in the carbohydrate metabolism of skeletal muscle (Ziel et al 1988). Reduction in insulin-mediated glucose uptake in diabetes has been reported (Berger et al 1989). In fact, insulin action is greater in the red type I fibres of soleus muscle (James et al 1985). With this in mind, we prepared soleus muscle samples from STZ-diabetic rats to evaluate the effect of tetrandrine on glucose uptake. We found that tetrandrine caused an increase in glucose uptake into soleus muscles isolated from STZ-diabetic rats. The effective dose of tetrandrine (1.0 mg kg^{-1}) required to lower the higher plasma glucose of STZ-diabetic rats was about 1.6 μmol L^{-1}, a value near to that (1.0 μmol L^{-1}) produced maximum effect on glucose uptake into soleus muscles. The results obtained therefore indicate that tetrandrine could increase the utilization of glucose in peripheral tissue to regulate glucose homeostasis via an insulin-independent mechanism.

Mammalian cells store glycogen in the liver for production of glucose 6-phosphate during glycolysis (Bollen et al 1998). Insulin deficiency is clearly associated with changes in hepatic metabolism (Hanson & Reshef 1997). Thus, we used liver samples to investigate the effect of tetrandrine on the incorporation of glucose into glycogen that can be related to the decrease in plasma glucose. Although not as effective as bovine insulin, tetrandrine markedly increased glycogen synthesis in hepatocytes isolated from diabetic rats. These results can be used to link the increase in glucose utilization by tetrandrine in peripheral tissue to the lowering of plasma glucose in an insulin-deficient state. However, the major mechanism of tetrandrine for lowering plasma glucose needs to be characterized in the future. It has been mentioned that long-term treatment of dogs with tetrandrine at the higher oral dose of 40.0 mg kg^{-1} may induce focal necrosis of liver cells (Tainlin et al 1982). However, a beneficial effect of tetrandrine at an oral dose of 10 mg kg^{-1} per day on experimental hepatic fibrosis induced by bile duct ligation and scission in rats has also been documented (Park et al 2000). In the present study, the dose of tetrandrine effective for lowering plasma glucose in STZ-diabetic rats is less than that required to produce these effects in the liver. Although tetrandrine was not as effective as bovine insulin in lowering plasma glucose in STZ-diabetic rats, our data showed that tetrandrine is useful as an attractive adjuvant for the handling of diabetic patients in the future. The oral pharmacological usefulness and potency of tetrandrine in the regulation of plasma glucose under the insulin deficient state will be investigated in the future.

It has been documented that the demethylation of the 7-O position and/or addition of a 2- or 2′-N-oxide side chain in bis-benzylisoquinoline compounds in Stephania has a role in the induction of anti-hyperglycemic actions in STZ-diabetic mice (Tsutsumi et al 2003). However, the compound of tetrandrine used in the present study is non-demethylated. This variation of the structure modification of tetrandrine on the plasma glucose lowering action might be related to the differences in animal species in the ddY and Wistar strains. It has also been reported that tetrandrine causes the death of malignant lymphoid and myeloid cells (Teh et al 1991). Tetrandrine seems to be a valuable anti-neoplastic agent. However, the apoptotic effect of tetrandrine linked to the plasma glucose lowering effect shall be investigated in the future.

Conclusions

The data obtained in this study suggest that intravenous injection of tetrandrine can lower plasma glucose in STZ-diabetic rats due to an increase of glucose utilization in peripheral tissues via non-insulin-mediated mechanisms.

References

Baron, A. D., Brechtel, G., Wallace, P., Edelman, S. V. (1988) Rates and tissue sites of non-insulin-and insulin-mediated glucose uptake in humans. *Am. J. Physiol.* **255**: E769–E774

Berger, J., Biswas, C., Vicario, P. P., Strout, H. V., Saperstein, R., Pilch, P. F. (1989) Decreased expression of the insulin-responsive glucose transporter in diabetes and fasting. *Nature* **340**: 70–72

Bessesen, D. H. (2001) The role of carbohydrates in insulin resistance. *J. Nutr.* **131**: 2782S–2786S

Bollen, M., Keppens, S., Stalmans, W. (1998) Specific features of glycogen metabolism in the liver. *Biochem. J.* **336**: 1–31

Cao, Z. F. (1996) Scavenging effect of tetrandrine of active oxygen radicals. *Planta Med.* **62**: 413–414

Cerielo, A., Motz, E., Cavarape, A., Lizzio, S., Russo, A., Quatraro, A., Giugliano, D. (1997) Hyperglycemia counterbalances the antihypertensive effect of glutathione in diabetic patients: evidence linking hypertension and glycemia through the oxidative stress in diabetes mellitus. *J. Diabetes Complicat.* **11**: 250–255

Cheng, J. T., Liu, I. M., Chi, T. C., Tzeng, T. F., Lu, F. H., Chang, C. J. (2001) Plasma glucose lowering effect of tramadol in streptozotocin-induced diabetic rats. *Diabetes* **50**: 2815–2821

Consoli, A., Nurjhan, N., Capani, F., Gerich, J. (1989) Predominant role of gluconeogenesis in increased hepatic glucose production in NIDDM. *Diabetes* **38**: 550–557

Felix, J. P., King, V. F., Shevell, J. L., Garcia, M. L., Kaczorowski, G. J., Bick, I. R., Slaughter, R. S. (1992) Bis(benzylisoquinoline) analogs of tetrandrine block L-type calcium channels: evidence for interaction at the diltiazem-binding site. *Biochemistry* **31**: 11793–11800

Hanson, R. W., Reshef, L. (1997) Regulation of phosphoenolpyruvate carboxykinase (GTP) gene expression. *Annu. Rev. Biochem.* **66**: 581–611

Hu, G. X., Hu, Y., Fang, D. C., Jiang, M. X. (1987) Hemodynamic effects of tetrandrine in conscious rats. *Acta. Pharmacol. Sin.* **8**: 325–328

Huang, Y. T., Hong, C. Y. (1998) Tetrandrine. *Cardiovasc. Drug Rev.* **16**: 1–15

James, D. E., Jenkins, A. B., Kraegen, E. W. (1985) Heterogeneity of insulin action in individual muscles in vivo: euglycemic clamp studies in rats. *Am. J. Physiol.* **248**: E567–E574

Kim, H. S., Zhang, Y. H., Oh, K. W., Ahn, H. Y. (1997) Vasodilating and hypotensive effects of fangchinoline and tetrandrine on the rat aorta and the stroke-prone spontaneously hypertensive rat. *J. Ethnopharmacol.* **58**: 117–123

Kosegawa, I., Chen, S., Awata, T., Negishi, K., Katayama, S. (1999) Troglitazone and metformin, but not glibenclamide, decrease blood pressure in Otsuka Long Evans Tokushima Fatty rats. *Clin. Exp. Hypertens.* **21**: 199–211

Lee, J. H., Kang, G. H., Kim, K. C., Kim, K. M., Park, D. I., Choi, B. T., Kang, H. S., Lee, Y. T., Choi, Y. H. (2002) Tetrandrine-induced cell cycle arrest and apoptosis in A549 human lung carcinoma cells. *Int. J. Oncol.* **21**: 1239–1244

Lieberman, I., Lentz, D. P., Trucco, G. A., Seow, W. K., Thong, Y. H. (1992) Prevention by tetrandrine of spontaneous development of diabetes mellitus in BB rats. *Diabetes* **41**: 616–619

Lopez-Candales, A. (2001) Metabolic syndrome X: a comprehensive review of the pathophysiology and recommended therapy. *J. Med.* **32**: 283–300

Park, P. H., Nan, J. X., Park, E. J., Kang, H. C., Kim, J. Y., Ko, G., Sohn, D. H. (2000) Effect of tetrandrine on experimental hepatic fibrosis induced by bile duct ligation and scission in rats. *Pharmacol. Toxicol.* **87**: 261–268

Shen, Y. C., Chen, C. F., Wang, S. Y., Sung, Y. J. (1999) Impediment to calcium influx and reactive oxygen production accounts for the inhibition of neutrophil Mac-1 up-regulation and adhesion by tetrandrine. *Mol. Pharmacol.* **55**: 186–193

Sun, G. R., Zhang, G. F., Wei, Y. J., Yang, D. S., Zhang, J. X., Tian, Z. B. (1994) Protective effect of tetrandrine on pancreatic islet cells damaged by alloxan in rats. *Acta. Pharmacol. Sin.* **46**: 161–167

Sutter, M. C., Wang, Y. X. (1993) Recent cardiovascular drugs from Chinese medicinal plants. *Cardiovasc. Res.* **27**: 1891–1901

Tainlin, L., Tingyi, H., Changqi, Z., Peipei, Y., Qiong, Z. (1982) Studies of the chronic toxicity of tetrandrine in dogs: an inhibitor of silicosis. *Ecotoxicol. Environm. Safety* **6**: 528–534

Teh, B. S., Chen, P., Lavin, M. F., Seow, W. K., Thong, Y. H. (1991) Demonstration of the induction of apoptosis (programmed cell death) by tetrandrine, a novel anti-inflammatory agent. *Int. J. Immunopharmacol.* **13**: 1117–1126

Tsutsumi, T., Kobayashi, S., Liu, Y. Y., Kontani, H. (2003) Anti-hyperglycemic effect of fangchinoline isolated from Stephania tetrandra Radix in streptozotocin-diabetic mice. *Biol. Pharm. Bull.* **26**: 313–317

Ziel, F. H., Venkatesan, N., Davidson, M. B. (1988) Glucose transport is rate limiting for skeletal muscle glucose metabolism in normal and STZ-induced diabetic rats. *Diabetes* **37**: 885–890

A Novel Adjuvant for Mucosal Immunity to HIV-1 gp120 in Nonhuman Primates[1]

Naoto Yoshino,[2]* Fabien X.-S. Lü,† Kohtaro Fujihashi,[3]* Yukari Hagiwara,* Kosuke Kataoka,* Ding Lu,† Linda Hirst,† Mitsuo Honda,‡ Frederik W. van Ginkel,* Yoshifumi Takeda,§ Christopher J. Miller,† Hiroshi Kiyono,*¶ and Jerry R. McGhee*

The development of a safe and effective mucosal adjuvant is a crucial step toward a mucosal HIV/AIDS vaccine. This study seeks to determine the promise of a nontoxic mutant of cholera toxin (mCT; E112K) as a mucosal adjuvant in nonhuman primates. HIV-1 gp120 was nasally administered together with mCT E112K or native CT (nCT) as adjuvant on five to six occasions over a 6- to 8-wk period to groups of four rhesus macaques and alone to two monkeys that acted as controls. Macaques given nasal gp120 with either mCT E112K or nCT showed elevated gp120-specific IgG and IgA Ab responses with virus-neutralizing activity in both their plasma and mucosal external secretions, as well as higher numbers of gp120-specific IgA Ab-forming cells in their mucosal and peripheral lymphoid tissues and of IL-4-producing Th2-type CD4-positive ($CD4^+$) T cells than did controls. Even though significant mucosal adjuvanticity was seen with both mCT E112K and nCT, neuronal damage was observed only in the nCT-treated, but not in the control or mCT E112K-treated groups. These results clearly show that mCT E112K is an effective and safe mucosal adjuvant for the development of a nasal HIV/AIDS vaccine. *The Journal of Immunology,* **2004, 173: 6850–6857.**

It is well known that HIV-1 infections occur through contact with contaminated blood or during unprotected vaginal or anal intercourse. Indeed, it is estimated that 70–85% of HIV-1 infections are transmitted sexually (1–3). Given that fact, immune responses at mucosal surfaces in which the virus crosses the epithelium of the genital or rectal tracts are an essential component of vaccine-induced protection. The evidence for an association between mucosal immune responses and protection in humans has stemmed from studies on the immune system of women who remained seronegative despite a high rate of exposure to HIV-1. High levels of secretory IgA were detected in the genital secretions of the protected women (4–7). Because the mucosa of the small and large intestine are the largest source of lymphocytes and APCs in the host (8, 9), they act as a potential reservoir for HIV-1-infected cells in viral pathogenesis (10). Studies to develop a HIV/AIDS mucosal vaccine have been conducted in nonhuman primate (NHP)[4] models by using recombinant SIV proteins or peptides (11–17), live-attenuated SIVs (18–23), SIV-encoded virus or bacterial vectors (24–29), DNA vaccines (30–33), and a prime/boost regimen (34–36). Collectively, these studies point to the importance of a mucosal HIV/AIDS vaccine for the prevention of HIV-1 infection.

Recent studies have shown that nasal immunization is the most effective approach for the induction of both mucosal and systemic immune responses (37). For example, nasal immunization with protein/peptide vaccines together with mucosal adjuvant more effectively induces mucosal immunity in the female reproductive tract than does oral immunization (38). Like its gut-associated lymphoreticular tissue counterpart in the gastrointestinal tract, the nasopharyngeal-associated lymphoreticular tissue-based immune system is key to the induction of Ag-specific mucosal and systemic immune responses (39–41). In this regard, we have shown that nasal immunization of rhesus macaques with SIV $p55^{gag}$ together with native cholera toxin (nCT) as mucosal adjuvant induced $p55^{gag}$-specific IgA and IgG Ab responses in vaginal secretions (16).

Although a potent mucosal adjuvant, nCT is not practical for use in humans because of its toxicity. Nasal application of CT B subunit (CT-B) or nCT resulted in its accumulation in the olfactory bulbs of the CNS through GM1 binding and in its subsequent retrograde axonal transport into the olfactory neurons (39). Furthermore, nCT is known to induce high levels of total and Ag-specific IgE Ab responses due to the nature of IL-4-dependent adjuvanticity (40–43). To overcome these potent pathological problems of nCT, we have developed and characterized two nontoxic mutants of cholera toxin (mCT; E112K and S61F) that retain adjuvant properties despite lacking the ADP-ribosyltransferase enzyme activity associated with toxicity (42, 43). Studies by our own group and by others have shown that mutant CT E112K is one of the most effective, safe, and stable adjuvants among the toxin-based mutants that have been tested (41–43).

*Departments of Oral Biology and Microbiology, Immunobiology Vaccine Center, University of Alabama, Birmingham, AL 35294; †California Regional Primate Research Center, Department of Pathology, School of Medicine, University of California, Davis, CA 95616; ‡AIDS Research Center, National Institute of Infectious Diseases, §Jissen Women's College, and ¶Division of Mucosal Immunology, Department of Microbiology and Immunology, Institute for Medical Sciences, University of Tokyo, Tokyo, Japan

Received for publication May 17, 2004. Accepted for publication September 9, 2004.

The costs of publication of this article were defrayed in part by the payment of page charges. This article must therefore be hereby marked *advertisement* in accordance with 18 U.S.C. Section 1734 solely to indicate this fact.

[1] This study was supported by U.S. Public Health Service Grants RR13149, AI 35932, AI 18958, DK 44240, AI 43197, DE 12242, and P30 DK 54781, and grants from the Ministry of Health and Labor, and the Ministry of Education, Science, Culture, and Sports, Core Research for Engineering, Science, and Technology-Japan Science and Technology Agency, Japan.

[2] Current address: Department of Microbiology, Iwate Medical University School of Medicine, 19-1, Uchimaru, Morioka 020-8505, Japan.

[3] Address correspondence and reprint requests to Dr. Kohtaro Fujihashi, Department of Oral Biology, School of Dentistry, Immunobiology Vaccine Center, University of Alabama at Birmingham, 761 Bevill Biomedical Research Building, 845 19th Street South, Birmingham, AL 35294-2170. E-mail address: kohtarof@uab.edu

[4] Abbreviations used in this paper: NHP, nonhuman primate; AFC, Ab-forming cell; LP, lamina propria; mCT, nontoxic mutant of cholera toxin; MLN, mesenteric lymph node; nCT, native cholera toxin; NGF, nerve growth factor; NP, nasal passage; SMG, submandibular gland.

0022-1767/04/$02.00

Because HIV-1 is most often transmitted via mucosal surfaces, a mucosal vaccine capable of inducing protective Abs and/or CTLs in mucosal tissues and external secretions would act as a first line of defense at the site of initial invasion. We take the first step toward the ultimate goal of developing a safe and effective mucosal adjuvant for a mucsoal HIV/AIDS vaccine in humans by assessing in this study the efficacy and safety of mCT E112K as a mucosal adjuvant in nonhuman primates.

Materials and Methods

HIV-1 immunogen and adjuvant used

HIV-1_{LAI} *Env* gp120 was kindly provided by Quality Biologicals (Gaithersburg, MD) through Contract N01-AI 65278 of the Vaccine Research and Development Branch, Division of AIDS, National Institute of Allergy and Infectious Diseases, National Institutes of Health. *Escherichia coli* strains containing the plasmids for the mCT E112K were grown in Luria-Bertani medium (10 mg/ml NaCl, 5 mg/ml yeast extract, 10 mg/ml tryptone) with 100 μg/ml ampicillin (42, 43). The mCT E112K was purified using a D-galactose-immobilized column (Pierce, Rockford, IL) from a cell suspension prepared by sonication of the recombinant *E. coli*, as described previously (42, 43). The purity of mCT E112K was assessed by SDS-PAGE, and no contaminating proteins were noted. The nCT was purchased from List Biological Laboratories (Campbell, CA).

Rhesus macaques

Five mature female and seven male rhesus macaques (*Macaca mulatta*), bred in captivity and reproductively cycling, were obtained from the California Regional Primate Research Center (Davis, CA). They were confirmed negative for Abs to HIV-2, SIV, type D retrovirus, and simian T cell lymphotropic virus-1 (STLV-1), and were maintained in conditions that fully complied with the standards of the American Association of Accreditation of Laboratory Animal Care at the California Regional Primate Research Center.

Immunization methods and schedule used

Rhesus macaques were divided into four groups and nasally immunized with vaccine containing: 1) 100 μg of gp120 alone, 2) 100 μg of gp120 plus 10 μg of nCT, 3) 100 μg of gp120 plus 25 μg of mCT E112K, or 4) 100 μg of gp120 plus 100 μg of mCT E112K. Macaques were anesthetized with ketamine and placed in dorsal recumbancy with head tilted back so that the nares were pointed upward (16). Vaccine solution (0.5 ml) was instilled dropwise into each nostril without inserting the syringe into the nasal cavity. Macaques were kept in that position for 10 min and then placed in lateral recumbancy until they recovered from anesthesia, as described previously (16). Nasal immunization was conducted on days 0, 7, 14, 28, 42, and 56.

Collection of peripheral blood, tissues, and external secretion samples and lymphocyte isolation

Tissues and peripheral blood were harvested using sterile techniques, and appropriate biohazard precautions were observed. The PBMCs were isolated from heparinized peripheral blood using Lymphocyte-Mammal (Cedarlane Laboratories, Hornby, Canada) (44). Plasma, vaginal washes consisting of a mixture of cervical and vaginal secretions, rectal washes, nasal washes, and saliva were collected, as previously described (16). These four external secretions along with the plasma were stored at −80°C until used for the analysis of gp120-specific Ab responses. For isolation of lymphocytes from different mucosal tissues, a modified enzymatic dissociation procedure was used (15, 16). Nasal passages (NP) and submandibular glands (SMG) were dissociated using collagenase type IV (0.5 mg/ml; Sigma-Aldrich, St. Louis, MO) in RPMI 1640 (Mediatech, Washington, DC) for 30 min at 37°C. After removal of Peyer's patches, the small intestine was treated first with PBS containing 1 mM DTT and then with 1 mM EDTA, while lamina propria (LP) mononuclear cells were isolated using the same method as for the NPs. The lymphocytes from tissues were purified using a discontinuous 40 and 75% Percoll gradient (Amersham Biosciences, Piscataway, NJ), as described previously (15, 16).

Monoclonal Abs

The mAbs used for cell surface staining in flow cytometric analysis were as follows: FITC-, PE-, or PerCP-conjugated mAb to human CD3 (SP34; BD Biosciences, San Jose, CA), CD4 (SK3; BD Biosciences), and CD8 (SK1; BD Biosciences). Cross-reactivity of these mAbs for the rhesus macaque was determined using the method described previously (45). However, the observed cross-reactivity with IL-5, IL-10, and IL-13 is a new finding and has not been published previously.

HIV-1 env *gp120-specific ELISA and ELISPOT assays*

HIV-1 *env* gp120-specific IgG, IgM, and IgA Ab titers in plasma, saliva, nasal washes, as well as rectal and vaginal lavages were determined by ELISA, as described previously (15, 16). The HIV-1 *env* gp120-specific IgG, IgM, and IgA Ab-forming cells (AFCs) were also determined by ELISPOT assay, as described elsewhere (15, 16).

Cytokine-specific ELISPOT assay

The PBMCs or lymphoid cells from various tissues were cultured in 10% FCS containing RPMI 1640 (Mediatech) supplemented with HEPES buffer (10 mM), L-glutamine (2 mM), nonessential amino acid solution (10 ml/L), sodium pyruvate (10 mM), penicillin (100 U/ml), streptomycin (100 μg/ml), and gentamicin (80 μg/ml) (complete medium) with or without 5 μg/ml HIV-1 *env* gp120, 1 μg/ml anti-human CD28 (CD28.2; BD Biosciences), and anti-human CD49d (9F10; BD Biosciences) mAbs at 37°C with 5% CO_2. Nonadherent cells were harvested after 3 days of incubation and stained with anti-human CD3 and CD8 mAbs. The FACSVantage (BD Biosciences) was used to sort out a subset of $CD3^+CD8^-$ T cells. The frequencies of $CD4^+$ Th1- and Th2-type cytokine-producing cells were determined by using rhesus macaque cytokine-specific ELISPOT kits (U-CyTech, Utrecht, The Netherlands).

In vitro HIV-1 neutralization assay

The diluted plasma or appropriate mucosal secretion was heat inactivated (56°C for 30 min) and incubated with 20 $TCID_{50}$ (50% tissue culture infective dose) units of HIV-1_{LAI} overnight at 4°C. This mixture was then cocultured with 1×10^6 M8166 cells for 2 h (16, 46, 47). After being washed twice with PBS, the cells were cultured in complete medium for 4 days at 37°C. Following incubation, culture supernatants were subjected to Lumipulse (chemiluminescence enzyme immunoassay/full automatic analyzer; Fujirebio, Tokyo, Japan) for measurement of HIV p24. The results were expressed as the percent inhibition of p24 *gag* production in culture supernatants when compared with the cultures containing pre- or nonimmunized plasma or mucosal secretions (16, 46, 47).

Nerve growth factor-β1 (NGF-β1) production in macaque olfactory tissues

The nasal turbinate region of the olfactory tissues was obtained from each macaque at the time of sacrifice. At the termination of the study, the nasal turbinate was perfused with PBS at 25°C. This was followed by perfusion with 100 ml of Zamboni's fixative (4% paraformaldehyde, 15% picric acid) in 0.1 M phosphate buffer. The olfactory bulbs and tubinates were removed and placed in fresh 4% paraformaldehyde at 4°C overnight. The tissue was then transferred to a 30% sucrose solution at 4°C for 48 h to cryoprotect it before sectioning. The tissue was then frozen in OCT compound, and the frozen sections (6 μm) were placed on precoated microscope slides (10% BSA in saline). For staining of sections, all slides were pretreated with rabbit IgG Ab to block nonspecific binding, followed by a biotinylated rabbit anti-human NGF-β1 Ab (Chemicon International, Temecula, CA) used at a concentration of 2 μg. The Ab-stained sections were incubated at 4°C overnight. The slides were then rinsed in three changes of PBS for 2 min and then reacted with avidin-biotin conjugate for 30 min at 25°C. The tissues were rinsed three times with PBS, and then reacted with 3,3′-diaminobenzidine (Vector Laboratories, Burlingame, CA) for 5–10 min before being again rinsed three times and having sections counterstained with hematoxylin for 30 s. After being washed in distilled water, the slides were dehydrated in 100% alcohol and xylene. In some experiments, the anti-NGF-β1 Ab-stained sections were incubated with HRP-conjugated streptavidin-Alexa Fluor 488 (Molecular Probes, Eugene, OR). Sections were examined with a fluorescence microscope (BX50/BXFLA; Olympus, Tokyo, Japan) equipped with a digital image capture system (Olympus).

Statistics

The results are expressed as the mean ± SEM. Immunized NHP groups were compared with the controls using a Mann-Whitney *U* test with Statview II software (Abacus Concepts, Berkeley, CA) designed for Macintosh computers. A p value of <0.05 or less was considered significant.

Results

Plasma anti-gp120-specific Ab responses

In this study, we have assessed the mucosal adjuvanticity of mCT E112K in rhesus macaques nasally immunized with HIV-1 gp120. Eleven macaques were given 100 μg of gp120 by the nasal route. In addition to the gp120, five macaques were given two doses of mCT E112K as nasal adjuvant, two (Rh09 and Rh91) receiving a 25 μg dose and three (NHPs Rh16, Rh39, and Rh85) receiving a 100 μg dose. As a positive control, and because our previous research showed that nCT is a potent nasal adjuvant for NHPs (16), four other macaques (Rh07, Rh35, Rh60, and Rh88) were given 10 μg of nCT along with gp120. As a negative control, the two remaining macaques (Rh43 and Rh51) were given gp120 alone. The gp120-specific IgG and IgA Abs in plasma of individual macaques were sequentially assessed by an endpoint ELISA. As expected based upon our previous studies (16), significant levels of gp120-specific IgG Ab responses were detected in plasma of all macaques given gp120 with nCT (Fig. 1; $p < 0.01$). Interestingly, comparable gp120-specific IgG Ab responses were observed in macaques receiving 100 μg of mCT E112K as nasal adjuvant (Fig. 1; $p < 0.01$), while much lower levels of these responses were noted in macaques receiving 25 μg of mCT E112K as nasal adjuvant ($p > 0.1$). Furthermore, the group receiving 100 μg of mCT E112K showed comparable gp120-specific plasma IgA Ab responses to those receiving nCT as mucosal adjuvant. In contrast, the two macaques given gp120 alone or those receiving only 25 μg of mCT E112K showed low to undetectable IgA Ab responses. When gp120-specific plasma Ab responses were compared between the two groups given 25 or 100 μg of mCT E112K groups, the group given the higher dose showed greater IgG ($p < 0.01$) and IgA Ab responses than did the group given 25 μg of mCT E112K. Taken together, these results show that 100 μg of mCT E112K is an appropriate dose for inducing HIV-1 gp120-specific plasma Ab responses.

Induction of gp120-specific mucosal immune responses

The gp120-specific IgA and IgG Ab titers were assessed in the mucosal secretions (saliva; nasal, vaginal, and rectal lavages) of macaques given nasal gp120 and mCT. The peak titers of IgG and IgA Abs occurred 7 or 14 days after the last nasal immunization

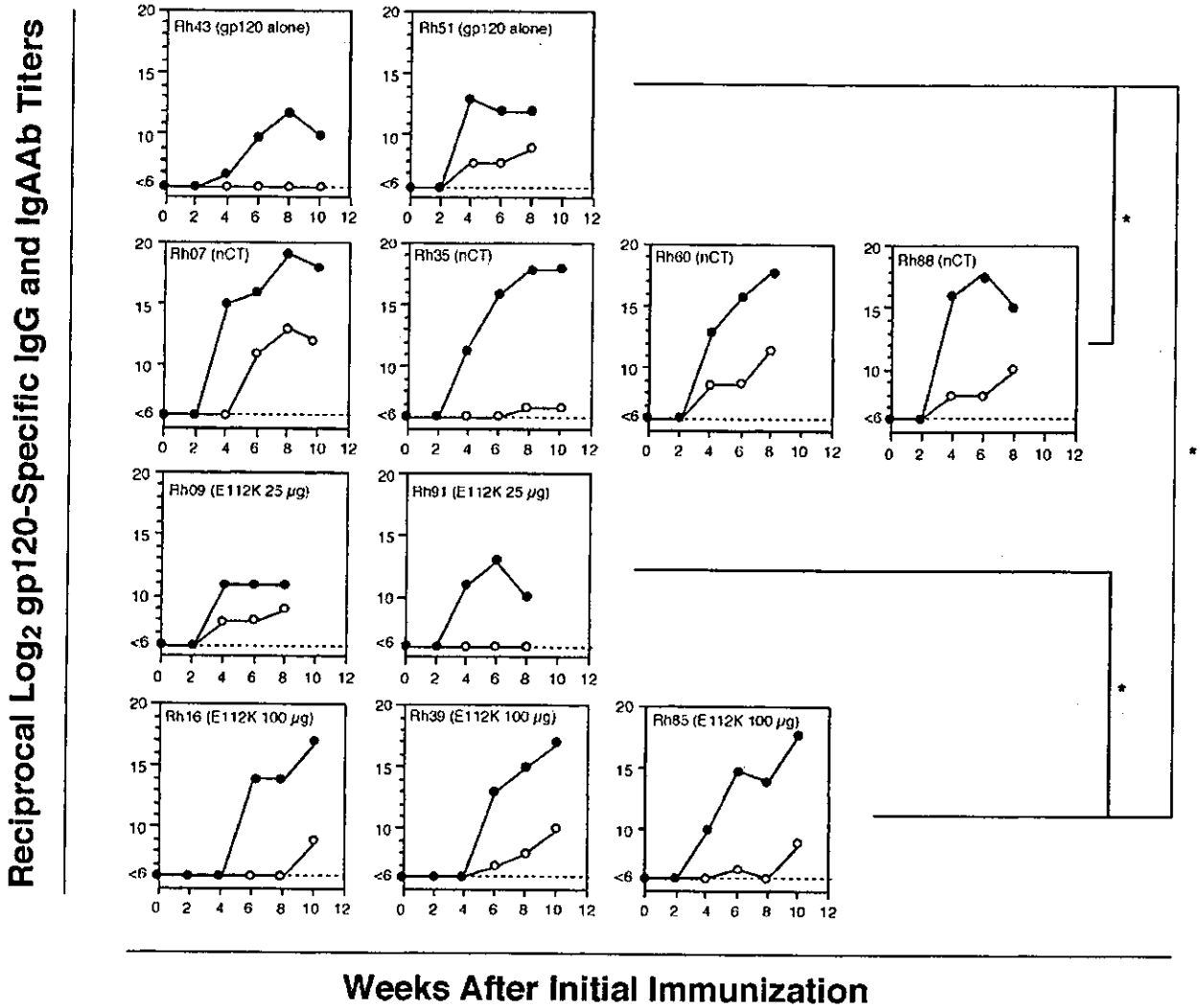

FIGURE 1. HIV-1 gp120-specific plasma IgG (●) and IgA (○) Ab titers were determined by endpoint ELISA. Rhesus macaques were nasally immunized with 100 μg of gp120 alone (Rh43 and Rh51), 100 μg of gp120 and 10 μg of nCT (Rh07, Rh35, Rh60, and Rh88), 100 μg of gp120 and 25 μg of mCT E112K (Rh09 and Rh91), or 100 μg of gp120 and 100 μg of mCT E112K (Rh16, Rh39, and Rh85). The data shown are endpoint titers for each macaque. *, $p < 0.01$ for IgG titers.

Table I. *gp120-specific Ab responses in mucosal secretions of rhesus macaques given a nasal vaccine*

Nasally Immunized with		Identification Number of Macaque	Anti-gp120-Specific Reciprocal Log_2 Ab Titers[a]							
			Saliva		Nasal washes		Vaginal washes		Rectal washes	
gp120	Adjuvant		IgA	IgG	IgA	IgG	IgA	IgG	IgA	IgG
100 (μg)	E112K (25 μg)	Rh09	<1[b]	2	NA[c]	NA	<1	3	NA	NA
		Rh91	2	2	NA	NA	<1	<1	NA	NA
	E112K (100 μg)	Rh16	6	5	5	3	NA	NA	3	<1
		Rh39	8	7	5	4	NA	NA	2	3
		Rh85	4	6	4	<1	NA	NA	3	<1
100 (μg)	nCT (10 μg)	Rh60	6	6	NA	NA	2	6	NA	NA
		Rh88	2	<1	NA	NA	<1	4	NA	NA
		Rh07	7	7	7	4	NA	NA	3	<1
		Rh35	5	5	2	<1	NA	NA	<1	<1
100 (μg)	None	Rh51	<1	<1	NA	NA	<1	2	NA	NA
		Rh43	3	2	<1	<1	NA	NA	<1	<1

[a] Saliva, nasal, vaginal, and rectal washes were collected 7 or 14 days after final immunization and were then subjected to gp120-specific ELISA.
[b] Endpoint titers were expressed as the last dilution giving an OD_{460} of 0.1 U above samples obtained from nonimmunized controls.
[c] NA, Not available.

(Table I). The findings for mucosal secretions paralleled those for plasma described above, with a dose of 100 μg of mCT E112K inducing gp120-specific IgA and IgG Ab levels comparable to those seen in macaques receiving nCT, but with a dose of only 25 μg of mCT E112K failing to support induction of gp120-specific Ab responses (Table I). These findings further support the notion that 100 μg of mCT E112K is the optimal dose for nasal adjuvanticity. Furthermore, our results demonstrate that a nasal vaccine of HIV-1 gp120 and mCT E112K as mucosal adjuvant would be an effective regimen for induction of anti-HIV-1 immune responses in external secretions of NHPs.

Induction of gp120-specific AFCs in mucosal lymphoid tissues

The induction of gp120-specific Ab responses was further confirmed at the level of plasma cell AFC responses. Comparable numbers of HIV-1 gp120-specific IgA and IgG AFCs were seen in the nasal passages of macaques immunized with gp120 plus either the optimal dose of mCT E112K (Rh39) or nCT (Rh60). Similarly, the numbers of gp120-specific IgA AFCs in SMGs and intestinal LP of macaques given the optimal dose of mCT E112K were comparable to those seen in positive controls given nCT as mucosal adjuvant (Fig. 2). These findings show that nasally coadministered mCT possesses adjuvant activity for the induction of gp120-specific AFCs in mucosal effector tissues.

gp120-specific $CD4^+$ Th1 and Th2 cell responses

Because nasal mCT showed adjuvant activity in both mucosal and systemic lymphoid compartments, HIV-1 gp120-specific $CD4^+$ Th1- and Th2-type responses were assessed using a cytokine-specific ELISPOT assay. When restimulated with gp120 in vitro, mononuclear cells from spleen and mesenteric lymph nodes (MLNs) of macaques immunized with gp120 and either mCT E112K or nCT induced both Th1 (IFN-γ)- and Th2-type (IL-4, IL-10, and IL-13) cytokine-producing $CD4^+$ T cells (Fig. 3). Both the group given mCT E112K and that given nCT showed higher numbers of IL-4- and IL-13-producing $CD4^+$ T cells in MLNs than those observed in the two macaques nasally immunized with gp120 alone. The nCT-immunized group exhibited higher numbers of IL-4- and IL-13-producing $CD4^+$ T cells than did the mCT E112K-immunized macaques, but the latter group showed higher numbers of IL-10-producing $CD4^+$ T cells were noted in their MLNs. A similar pattern of Th2-type cytokine production was seen in the spleens of these two groups of macaques. The IFN-γ-producing $CD4^+$ T cells were also seen in both MLNs and spleens

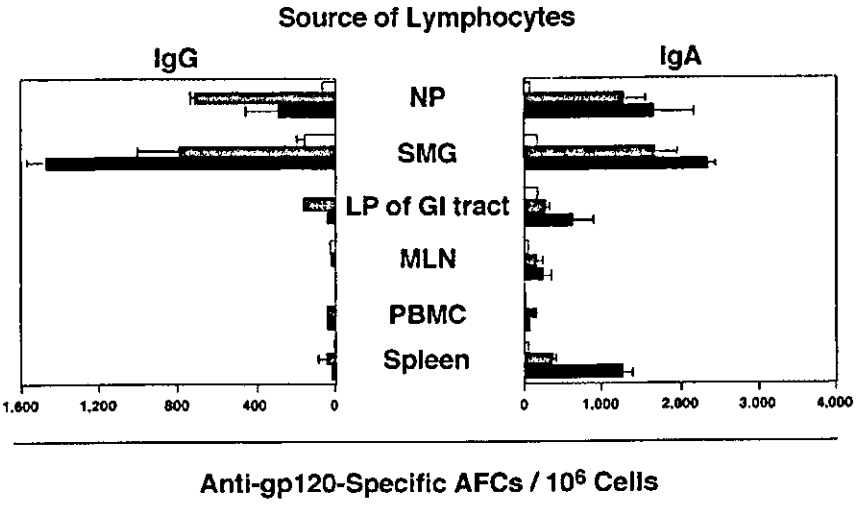

FIGURE 2. The gp120-specific IgG and IgA AFCs in mucosal and systemic lymphoid tissues of rhesus macaques (Rh51, □; Rh60, □; Rh39, ■) were determined by ELISPOT assay. Mononuclear cells were isolated from NPs, SMGs, the LP of the gastrointestinal tract; MLNs; spleen; and PBMC 2 wk following the final immunization. The results shown are the mean AFCs/10^6 cells ± SEM.

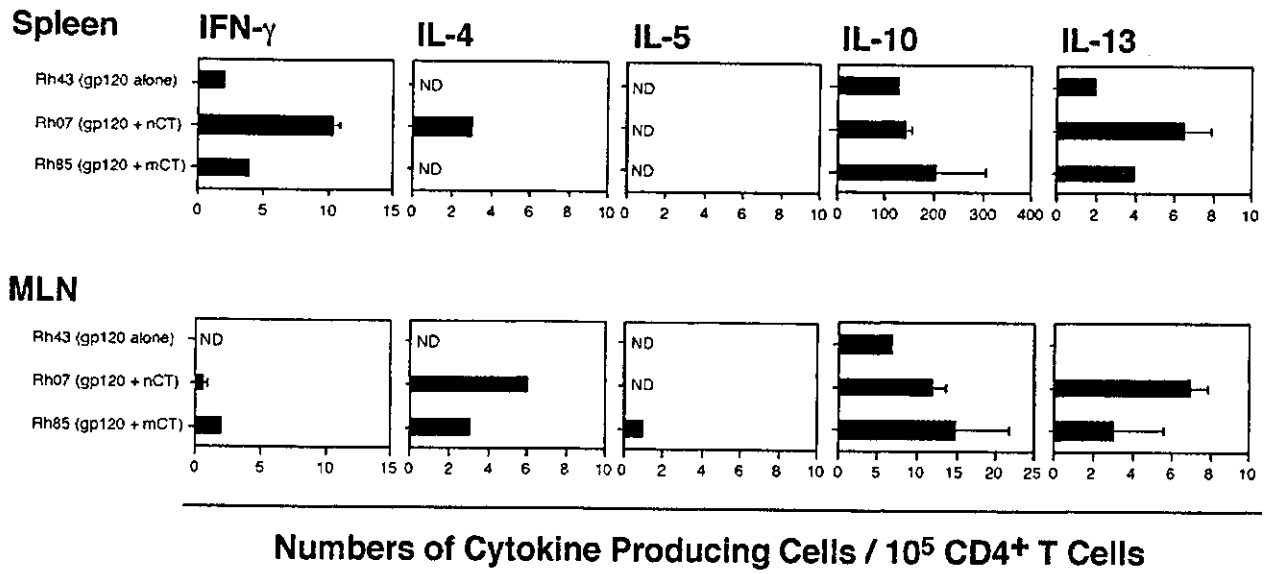

FIGURE 3. Th1 and Th2 cytokine production by gp120-stimulated $CD4^+$ T cells isolated from spleens and MLNs of rhesus macaques (Rh43, Rh07, and Rh85). Lymphocytes were cultured with or without gp120 for 3 days. Nonadherent cells were harvested and stained with anti-human CD3 and CD8 mAbs. A subset of $CD3^+$, $CD8^-$ T cells was purified using flow cytometry. The purified $CD4^+$ T cells were subjected to an array of macaque-specific cytokine (IFN-γ, IL-4, IL-5, IL-10, and IL-13) ELISPOT assays.

of macaques given either mCT E112K or nCT as mucosal adjuvant. Interestingly, the numbers of IFN-γ-producing $CD4^+$ T cells in the MLNs of both groups were lower than those seen in the spleens. These results suggest that mCT as nasal adjuvant preferentially induces Ag-specific Th2-type cytokine-producing $CD4^+$ T cells, while also somewhat enhancing the induction of Th1-type cytokine-producing $CD4^+$ T cells.

$HIV\text{-}1_{LAI}$-neutralizing Abs in external secretions and plasma

It was important to examine whether gp120-specific Abs in external secretions or plasma induced in NHPs given nasal gp120 and mCT E112K as mucosal adjuvant possessed HIV-neutralizing activity. To assess neutralizing activity, we performed an in vitro neutralization assay using $HIV\text{-}1_{LAI}$. The plasma (1/10 dilution) from macaques given nasal gp120 plus mCT E112K showed ~75–90% inhibition of $HIV\text{-}1_{LAI}$, a significantly higher rate than that seen in control plasma samples from either naive macaques or NHPs given gp120 only (Fig. 4*A*). Furthermore, the nasal lavages (1/10 dilution) from two rhesus macaques (Rh16 and Rh85) given nasal gp120 plus mCT E112K exhibited 35 and 55% inhibition of $HIV\text{-}1_{LAI}$, a rate of inhibition comparable to that seen in NHPs given nasal nCT as mucosal adjuvant. In contrast, control groups (naive macaques or those given gp120 alone) possessed little ability to inhibit $HIV\text{-}1_{LAI}$ (<20%) (Fig. 4*B*). These results clearly show that nontoxic mCT E112K can be used as a mucosal adjuvant for the induction of HIV-1-specific neutralizing immunity in both external secretions and plasma.

Safety of mCT E112K when used as a nasal adjuvant in NHPs

To assess the threat of neuronal damage posed by nasal vaccines containing gp120 and mCT E112K, NGF-β1 production in nasal turbinates of olfactory tissues was examined. Macaques given gp120 with nCT exhibited areas of intense NGF-β1 production in the olfactory region, which was associated with neuronal damage

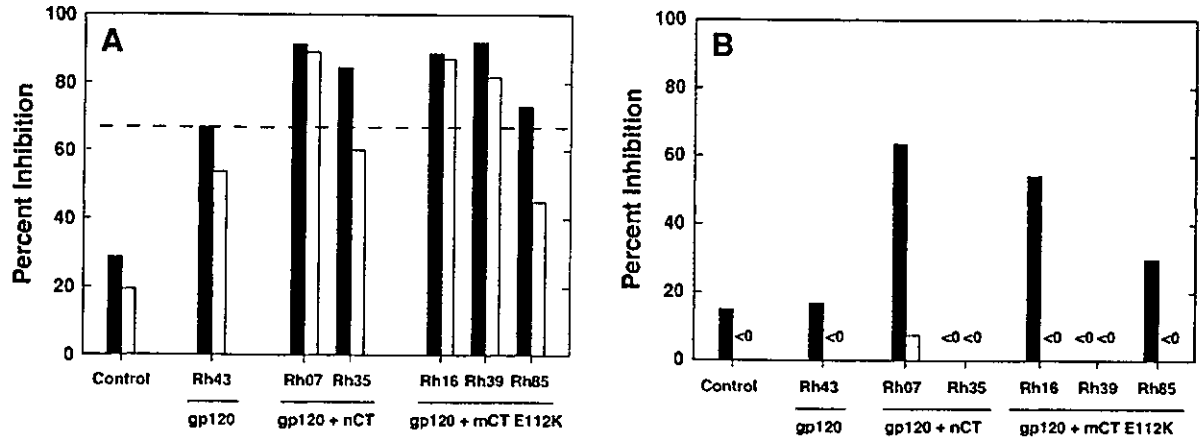

FIGURE 4. In vitro neutralization of HIV-1 was performed with a standard p24 release assay. The plasma (*A*) and nasal wash (*B*) samples were collected 2 wk after the final immunization. Samples were diluted 1/10 (■) or 1/100 (□) and were analyzed for the presence of neutralizing Abs against a homogenous laboratory strain ($HIV\text{-}1_{LAI}$). As controls, plasma samples were obtained from macaques before nasal immunization (preimmune sample). The results are the mean values of three separate assays.

and inhibition of apoptosis (Fig. 5*C*). In contrast, macaques given nasal gp120 plus mCT E112K (Fig. 5*B*) expressed very minimal levels of NGF-β1, which were essentially the same as those seen in olfactory tissues taken from the macaques given nasal gp120 alone (Fig. 5*A*). These results indicate that mCT E112K, although as effective a mucosal adjuvant as nCT, possesses none of its toxicity for neuronal tissues. As a safe and potent mucosal adjuvant, mCT E112K could speed the development of a nasal HIV-1 vaccine in humans.

Discussion

This study clearly provides direct evidence that mCT E112K is an effective mucosal adjuvant for the induction of HIV-1-specific immunity in the NHP model. When used as a nasal adjuvant, mCT E112K induced gp120-specific Abs possessing HIV-neutralizing activity in both external secretions and plasma, but showed negligible toxicity for the CNS-associated tissues of rhesus macaques. In contrast, nCT elicited increases in NGF-β production, a major manifestation of CNS inflammation. Thus, our study is the first to provide evidence establishing the efficacy and safety of an adjuvant for use in higher mammals. Collectively, our findings convincingly demonstrate the potential of mCT E112K as a mucosal adjuvant in humans and suggest that it may be time to take the next step toward the development of nasal vaccines, including those for HIV-1, by beginning clinical trials.

Our previous studies have already shown the efficacy and safety of mCT E112K as a nasal adjuvant in the murine system (43, 47, 48). In our earlier studies, we established that nasal immunization with pneumococcal surface protein A or diphtheria toxoid plus mCT E112K elicited sufficient Ag-specific immune responses to provide protection after lethal challenge with either *Streptococcus pneumoniae* bacteria or diphtheria exotoxin (48, 49). Furthermore, nasal application of mCT together with protein Ags elicited both Ag-specific IgA and IgG Ab responses in mucosal and systemic lymphoid tissue compartments (43, 47, 48). Among the different forms of mutant toxin-based adjuvants, mCT E112K was shown to be the safest and most effective in the murine model (41–43). However, until now, no studies assessing the mucosal adjuvanticity of different forms of toxin-based mutant adjuvants such as our mCT E112K had been performed in a large mammalian animal model, i.e., NHPs. Among the mammalian models, we chose the NHP experimental model as the most appropriate to and useful for the development of an HIV/AIDS mucosal vaccine.

AIDS is well known to be a sexually transmitted disease caused by HIV-1 infection via mucosal surfaces. The NHP experimental model of SIV infection has provided detailed evidence for the mucosal transmission of the virus, and has shown that the inhibition of its entry via the mucosa led to protection against disease development (50). Accordingly, an effective HIV/AIDS vaccine will be more readily developed if the potential of the common mucosal immune system is tapped, because mucosal immunization is known to induce effective protection against pathogens at mucosal surfaces as well as in lymphoid tissue compartments (37, 38, 51). Of note, our previous study showed that nasal immunization with SIV $p55^{gag}$ plus nCT as mucosal adjuvant induced in vaginal secretions of rhesus macaques Ag-specific Ab responses with virus-specific neutralizing Ab activity. In the case of the NHP experimental model, our studies have shown that mucosal (both oral or nasal) immunization with SIV $p55^{gag}$ plus nCT induced Ag-specific humoral and cellular immunity in both mucosal and systemic immune systems of rhesus macaques (15, 16, 52).

Despite its strong mucosal adjuvanticity, nCT is of little practical value as a mucosal adjuvant in humans because of its toxicity. Thus, much effort has been expended on the creation of genetically manipulated nontoxic mutants of CT that would retain adjuvanticity, but not toxicity. In the current study, we sought to examine the mucosal adjuvanticity of mCT E112K as nasal adjuvant when coadministered to rhesus macaques with HIV-1 gp120. In this study, we provide the first evidence that the nasal application of mCT E112K as a mucosal adjuvant effectively induces HIV-1 gp120-specific Ab responses in both mucosal and systemic lymphoid tissues of rhesus macaques. Furthermore, plasma and nasal

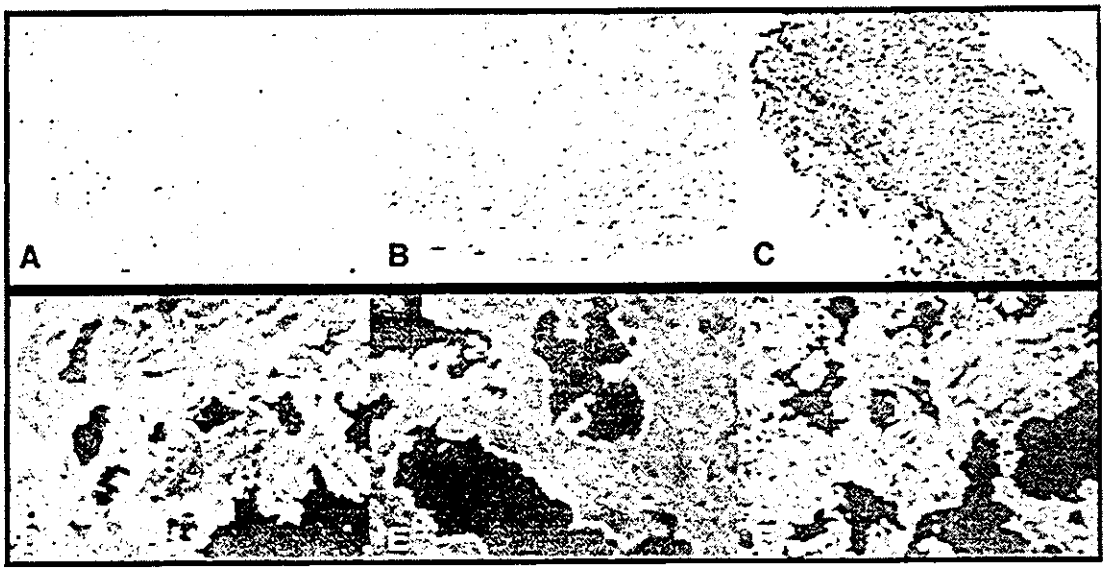

FIGURE 5. Detection of NGF-β1 expression in olfactory bulbs of rhesus macaques nasally immunized with gp120 and either nCT or mCT E112K as mucosal adjuvant. The anti-NGF-β1 Ab-stained sections were reacted with avidin-biotin conjugate, followed by 3,3′-diaminobenzidine (*A–C*), or incubated with HRP-conjugated streptavidin-Alexa Fluor 488 (*D–F*). *C* (×40) and *F* (×100), Show high expression of NGF-β1 along neuronal tracts when rhesus macaques were given nCT and gp120. *B* (×40) and *D* (×100), Show tissues from a macaque given gp120 plus mCT E112K. *A* (×40) and *D* (×100), Illustrate tissues from a macaque given gp120 alone.

washes from macaques given nasal gp120 plus mCT E112K contained HIV-1_{LAI}-neutralizing Abs. These findings clearly demonstrate the efficacy of mCT E112K as a mucosal adjuvant and suggest its potential for use in trial vaccines in humans.

However, nCT and even some of its nontoxic mutant forms pose additional, more specialized dangers when administered via the nasal route, the route of choice for mucosal vaccines because of its efficacy at inducing Ag-specific immune responses. Nasal vaccines using either nCT or one of its nontoxic mutants as adjuvant risk entering the CNS because of the proximity of the olfactory nerves/epithelium and olfactory bulbs to the brain. This potential for neurotoxicity has been a major obstacle for the use of enterotoxin-based mucosal adjuvants, even nontoxic mutant forms, in humans via the nasal route.

Our own studies have shown the potential toxicity of nCT for the olfactory nerves/epithelium and olfactory bulbs (39). Thus, neuronal association of CT-B through GM1 ganglioside binding appears to preclude efficient clearing of these enterotoxin-based mucosal adjuvants and to cause extended accumulation of them in neuronal tissues associated with the olfactory tract (39). These results show that nasally administered CT derivatives retain some toxicity and are targeted to the CNS, posing a serious obstacle to human use. Indeed, recent reports showed that a human vaccine containing inactivated influenza and native labile toxin as an adjuvant resulted in a very high incidence of Bell's palsy (53, 54). These results strongly indicate that it is essential to develop a more safe and effective nasal vaccine for human use.

Our current findings demonstrate the promise of the nontoxic form of mCT E112K as a safe and effective mucosal adjuvant and so point the way to the development of better nasal vaccines. The nontoxic form of mCT E112K did not elicit any increase in NGF-β expression by the olfactory tissues of NHPs. Only minimal NGF-β1 synthesis, comparable to that seen in NHP given nasal gp120 alone, was detected in the olfactory CNS tissues of rhesus macaques given nasal mCT E112K as nasal adjuvant.

Our previous study showed that nasal immunization with $p55^{gag}$ plus nCT induced $p55^{gag}$-specific T cell responses in both mucosal and systemic lymphoid tissue compartments (16). Thus, it was shown that both IFN-γ and IL-2 (Th1-type) expression as well as IL-5, IL-6, and IL-10 (Th2-type) production were seen in Ag-stimulated $CD4^+$ T cells isolated from NHPs given nasal $p55^{gag}$ and nCT. In this regard, our current study has shown that both Th1 (IFN-γ)- and Th2 (IL-10 and IL-13)-type cytokine-producing $CD4^+$ T cells were present in the MLNs and spleens of rhesus macaques given either mCT E112K or nCT as a nasal adjuvant. Although the viral Ags used in the current study are different from those in the previous report, our results also showed that mCT E112K provided adjuvanticity in NHPs through the generation of both Th1- and Th2-type cytokine responses by $CD4^+$ T cells. Induction of IFN-γ-producing $CD4^+$ T cells by nasally coadministered mCT E112K may be an additional benefit because it may lead to the generation of Ag-specific cell-mediated immunity responses. In viral infections including HIV and SIV, CTL activity has been shown to be of central importance for host defense and to correlate well with IFN-γ production (44). In this regard, we postulate that nasally coadministered mCT E112K would also induce CTL activity in various mucosal tissues. Confirming this prediction, rhesus macaques given nasal nCT as mucosal adjuvant showed SIV-specific CTL activity (16). We are currently testing Ag-specific CTL activity in macaques given nasal mCT E112K as mucosal adjuvant.

In conclusion, the current study has provided significant new information for a potential human phase I clinical trial using the nontoxic form of toxin mucosal adjuvant mCT E112K. Thus, nasal immunization of rhesus macaques with gp120 and mCT E112K resulted in the induction of Ab-neutralizing immunity against HIV-1 by inducing gp120-specific IgA and IgG Abs in both mucosal and systemic lymphoid tissue compartments, respectively. Furthermore, the safety of nasal mCT E112K was confirmed by the lack of CNS damage in this NHP model. This important new evidence supports the candidacy of mCT E112K as a potentially important mucosal adjuvant for use in humans.

Acknowledgments

We thank Dr. Kimberly K. McGhee for editorial comments on this manuscript. We also thank Sheila D. Turner for the final preparation of the paper.

References

1. Alexander, N. J. 1990. Sexual transmission of human immunodeficiency virus: virus entry into the male and female genital tract: World Health Organization, Global Program on Acquired Immune Deficiency Syndrome. *Fertil. Steril. 54:1.*
2. De Schryver, A., and A. Meheus. 1990. Epidemiology of sexually transmitted diseases: the global picture. *Bull. W. H. O. 68:639.*
3. Hospedales, J. 1989. Heterosexual spread of HIV infection. *Rev. Infect. Dis. 1:663.*
4. Mazzoli, S., D. Trabattoni, S. Lo Caputo, S. Piconi, C. Ble, F. Meacci, S. Ruzzante, A. Salvi, F. Semplici, R. Longhi, et al. 1997. HIV-specific mucosal and cellular immunity in HIV-seronegative partners of HIV-seropositive individuals. *Nat. Med. 3:1250.*
5. Kaul, R., D. Trabattoni, J. J. Bwayo, D. Arienti, A. Zagliani, F. M. Mwangi, C. Kariuki, E. N. Ngugi, K. S. MacDonald, T. B. Ball, et al. 1999. HIV-1-specific mucosal IgA in a cohort of HIV-1-resistant Kenyan sex workers. *AIDS 13:23.*
6. Devito, C., J. Hinkula, R. Kaul, L. Lopalco, J. J. Bwayo, F. Plummer, M. Clerici, and K. Broliden. 2000. Mucosal and plasma IgA from HIV-exposed seronegative individuals neutralize a primary HIV-1 isolate. *AIDS 14:1917.*
7. Kaul, R., F. Plummer, M. Clerici, M. Bomsel, L. Lopalco, and K. Broliden. 2001. Mucosal IgA in exposed, uninfected subjects: evidence for a role in protection against HIV infection. *AIDS 15:431.*
8. Brandtzaeg, P. 1989. Overview of the mucosal immune system. *Curr. Top. Microbiol. Immunol. 146:13.*
9. Lee, S. H., P. M. Starkey, and S. Gordon. 1985. Quantitative analysis of total macrophage content in adult mouse tissues: immunochemical studies with monoclonal antibody F4/80. *J. Exp. Med. 161:475.*
10. Smith, P. D., G. Meng, G. M. Shaw, and L. Li. 1997. Infection of gastrointestinal tract macrophages by HIV-1. *J. Leukocyte Biol. 62:72.*
11. Lehner, T., L. A. Bergmeier, C. Panagiotidi, L. Tao, R. Brookes, L. S. Klavinskis, P. Walker, J. Walker, R. G. Ward, L. Hussain, et al. 1992. Induction of mucosal and systemic immunity to a recombinant simian immunodeficiency viral protein. *Science 258:1365.*
12. Lehner, T., R. Brookes, C. Panagiotidi, L. Tao, L. S. Klavinskis, J. Walker, P. Walker, R. Ward, L. Hussain, J. H. Gearing, et al. 1993. T- and B-cell functions and epitope expression in nonhuman primates immunized with simian immunodeficiency virus antigen by the rectal route. *Proc. Natl. Acad. Sci. USA 90:8638.*
13. Lehner, T., L. Tao, C. Panagiotidi, L. S. Klavinskis, R. Brookes, L. Hussain, N. Meyers, S. E. Adams, A. J. Gearing, and L. A. Bergmeier. 1994. Mucosal model of genital immunization in male rhesus macaques with a recombinant simian immunodeficiency virus p27 antigen. *J. Virol. 68:1624.*
14. Lehner, T., Y. Wang, M. Cranage, L. A. Bergmeier, E. Mitchell, L. Tao, G. Hall, M. Dennis, N. Cook, R. Brookes, et al. 1996. Protective mucosal immunity elicited by targeted iliac lymph node immunization with a subunit SIV envelope and core vaccine in macaques. *Nat. Med. 2:767.*
15. Kubota, M., C. J. Miller, K. Imaoka, S. Kawabata, K. Fujihashi, J. R. McGhee, and H. Kiyono. 1997. Oral immunization with simian immunodeficiency virus $p55^{gag}$ and cholera toxin elicits both mucosal IgA and systemic IgG immune responses in nonhuman primates. *J. Immunol. 158:5321.*
16. Imaoka, K., C. J. Miller, M. Kubota, M. B. McChesney, B. Lohman, M. Yamamoto, K. Fujihashi, K. Someya, M. Honda, J. R. McGhee, and H. Kiyono. 1998. Nasal immunization of nonhuman primates with simian immunodeficiency virus $p55^{gag}$ and cholera toxin adjuvant induces Th1/Th2 help for virus-specific immune responses in reproductive tissues. *J. Immunol. 161:5952.*
17. Belyakov, I. M., Z. Hel, B. Kelsall, V. A. Kuznetsov, J. D. Ahlers, J. Nacsa, D. I. Watkins, T. M. Allen, A. Sette, J. Altman, et al. 2001. Mucosal AIDS vaccine reduces disease and viral load in gut reservoir and blood after mucosal infection of macaques. *Nat. Med. 7:1320.*
18. Lohman, B. L., M. B. McChesney, C. J. Miller, M. Otsyula, C. J. Berardi, and M. L. Marthas. 1994. Mucosal immunization with a live, virulence-attenuated simian immunodeficiency virus (SIV) vaccine elicits antiviral cytotoxic T lymphocytes and antibodies in rhesus macaques. *J. Med. Primatol. 23:95.*
19. Quesada-Rolander, M., B. Makitalo, R. Thorstensson, Y. J. Zhang, E. Castanos-Velez, G. Biberfeld, and P. Putkonen. 1996. Protection against mucosal SIVsm challenge in macaques infected with a chimeric SIV that expresses HIV type 1 envelope. *AIDS Res. Hum. Retroviruses 12:993.*
20. Nilsson, C., B. Makitalo, R. Thorstensson, S. Norley, D. Binninger-Schinzel, M. Cranage, E. Rud, G. Biberfeld, and P. Putkonen. 1998. Live attenuated simian

immunodeficiency virus (SIV)mac in macaques can induce protection against mucosal infection with SIVsm. *AIDS 12:2261.*
21. Johnson, R. P., J. D. Lifson, S. C. Czajak, K. S. Cole, K. H. Manson, R. Glickman, J. Yang, D. C. Montefiori, R. Montelaro, M. S. Wyand, and R. C. Desrosiers. 1999. Highly attenuated vaccine strains of simian immunodeficiency virus protect against vaginal challenge: inverse relationship of degree of protection with level of attenuation. *J. Virol. 73:4952.*
22. Enose, Y., M. Ui, A. Miyake, H. Suzuki, H. Uesaka, T. Kuwata, J. Kunisawa, H. Kiyono, H. Takahashi, T. Miura, and M. Hayami. 2002. Protection by intranasal immunization of a *nef*-deleted, nonpathogenic SHIV against intravaginal challenge with a heterologous pathogenic SHIV. *Virology 298:306.*
23. Shacklett, B. L., K. E. Shaw, L. A. Adamson, D. T. Wilkens, C. A. Cox, D. C. Montefiori, M. B. Gardner, P. Sonigo, and P. A. Luciw. 2002. Live, attenuated simian immunodeficiency virus SIVmac-M4, with point mutations in the Env transmembrane protein intracytoplasmic domain, provides partial protection from mucosal challenge with pathogenic SIVmac251. *J. Virol. 76:11365.*
24. Buge, S. L., E. Richardson, S. Alipanah, P. Markham, S. Cheng, N. Kalyan, C. J. Miller, M. Lubeck, S. Udem, J. Eldridge, and M. Robert-Guroff. 1997. An adenovirus-simian immunodeficiency virus *env* vaccine elicits humoral, cellular, and mucosal immune responses in rhesus macaques and decreases viral burden following vaginal challenge. *J. Virol. 71:8531.*
25. Benson, J., C. Chougnet, M. Robert-Guroff, D. Montefiori, P. Markham, G. Shearer, R. C. Gallo, M. Cranage, E. Paoletti, K. Limbach, et al. 1998. Recombinant vaccine-induced protection against the highly pathogenic simian immunodeficiency virus SIV(mac251): dependence on route of challenge exposure. *J. Virol. 72:4170.*
26. Crotty, S., B. L. Lohman, F. X. Lu, S. Tang, C. J. Miller, and R. Andino. 1999. Mucosal immunization of cynomolgus macaques with two serotypes of live poliovirus vectors expressing simian immunodeficiency virus antigens: stimulation of humoral, mucosal, and cellular immunity. *J. Virol. 73:9485.*
27. Leung, N. J., A. Aldovini, R. Young, M. A. Jarvis, J. M. Smith, D. Meyer, D. E. Anderson, M. P. Carlos, M. B. Gardner, and J. V. Torres. 2000. The kinetics of specific immune responses in rhesus monkeys inoculated with live recombinant BCG expressing SIV Gag, Pol, Env, and Nef proteins. *Virology 268:94.*
28. Crotty, S., C. J. Miller, B. L. Lohman, M. R. Neagu, L. Compton, D. Lu, F. X. Lu, L. Fritts, J. D. Lifson, and R. Andino. 2001. Protection against simian immunodeficiency virus vaginal challenge by using Sabin poliovirus vectors. *J. Virol. 75:7435.*
29. Izumi, Y., Y. Ami, K. Matsuo, K. Someya, T. Sata, N. Yamamoto, and M. Honda. 2003. Intravenous inoculation of replication-deficient recombinant vaccinia virus DIs expressing simian immunodeficiency virus *gag* controls highly pathogenic simian-human immunodeficiency virus in monkeys. *J. Virol. 77:13248.*
30. Wang, S. W., P. A. Kozlowski, G. Schmelz, K. Manson, M. S. Wyand, R. Glickman, D. Montefiori, J. D. Lifson, R. P. Johnson, M. R. Neutra, and A. Aldovini. 2000. Effective induction of simian immunodeficiency virus-specific systemic and mucosal immune responses in primates by vaccination with proviral DNA producing intact but noninfectious virions. *J. Virol. 74:10514.*
31. Gorelick, R. J., J. D. Lifson, J. L. Yovandich, J. L. Rossio, M. Piatak, Jr., A. J. Scarzello, W. B. Knott, J. W. Bess, Jr., B. A. Fisher, B. M. Flynn, et al. 2000. Mucosal challenge of *Macaca nemestrina* with simian immunodeficiency virus (SIV) following SIV nucleocapsid mutant DNA vaccination. *J. Med. Primatol. 29:209.*
32. Fuller, D. H., P. A. Rajakumar, L. A. Wilson, A. M. Trichel, J. T. Fuller, T. Shipley, M. S. Wu, K. Weis, C. R. Rinaldo, J. R. Haynes, and M. Murphey-Corb. 2002. Induction of mucosal protection against primary, heterologous simian immunodeficiency virus by a DNA vaccine. *J. Virol. 76:3309.*
33. Muthumani, K., M. Bagarazzi, D. Conway, D. S. Hwang, K. Manson, R. Ciccarelli, Z. Israel, D. C. Montefiori, K. Ugen, N. Miller, et al. 2003. A Gag-Pol/Env-Rev SIV239 DNA vaccine improves CD4 counts, and reduces viral loads after pathogenic intrarectal SIV251 challenge in rhesus macaques. *Vaccine 21:629.*
34. Amara, R. R., F. Villinger, J. D. Altman, S. L. Lydy, S. P. O'Neil, S. I. Staprans, D. C. Montefiori, Y. Xu, J. G. Herndon, L. S. Wyatt, et al. 2001. Control of a mucosal challenge and prevention of AIDS by a multiprotein DNA/MVA vaccine. *Science 292:69.*
35. Amara, R. R., J. M. Smith, S. I. Staprans, D. C. Montefiori, F. Villinger, J. D. Altman, S. P. O'Neil, N. L. Kozyr, Y. Xu, L. S. Wyatt, et al. 2002. Critical role for Env as well as Gag-Pol in control of a simian-human immunodeficiency virus 89.6P challenge by a DNA prime/recombinant modified vaccinia virus Ankara vaccine. *J. Virol. 76:6138.*
36. Dale, C. J., X. S. Liu, R. De Rose, D. F. Purcell, J. Anderson, Y. Xu, G. R. Leggatt, I. H. Frazer, and S. J. Kent. 2002. Chimeric human papilloma virus-simian/human immunodeficiency virus virus-like-particle vaccines: immunogenicity and protective efficacy in macaques. *Virology 301:176.*
37. McGhee, J. R., and H. Kiyono. 1998. The mucosal immune system. In *Fundamental Immunology*, 4th Ed. W. E. Paul, ed. Academic Press, San Diego, p. 909.
38. Fujihashi, K, and J. R. McGhee. The mucosal immune response. In *Topley and Wilson's Microbiology and Microbial Infections*. S. H. E. Kaufmann, ed. Edward Arnold, London, *In press.*
39. Van Ginkel, F. W., R. J. Jackson, Y. Yuki, and J. R. McGhee. 2000. The mucosal adjuvant cholera toxin redirects vaccine proteins into olfactory tissues. *J. Immunol. 165:4778.*
40. Xu-Amano, J., H. Kiyono, R. J. Jackson, H. F. Staats, K. Fujihashi, P. D. Burrows, C. O. Elson, S. Pillai, and J. R. McGhee. 1993. Helper T cell subsets for immunoglobulin A responses: oral immunization with tetanus toxoid and cholera toxin as adjuvant selectively induces Th2 cells in mucosa associated tissues. *J. Exp. Med. 178:1309.*
41. Okahashi, N., M. Yamamoto, J. L. Van Cott, S. N. Chatfield, M. Roberts, H. Bluethmann, T. Hiroi, H. Kiyono, and J. R. McGhee. 1996. Oral immunization of interleukin-4 (IL-4) knockout mice with a recombinant *Salmonella* strain or cholera toxin reveals that $CD4^+$ Th2 cells producing IL-6 and IL-10 are associated with mucosal immunoglobulin A responses. *Infect. Immun. 64:1516.*
42. Yamamoto, S., Y. Takeda, M. Yamamoto, H. Kurazono, K. Imaoka, M. Yamamoto, K. Fujihashi, M. Noda, H. Kiyono, and J. R. McGhee. 1997. Mutants in the ADP-ribosyltransferase cleft of cholera toxin lack diarrheagenicity but retain adjuvanticity. *J. Exp. Med. 185:1203.*
43. Yamamoto, S., H. Kiyono, M. Yamamoto, K. Imaoka, K. Fujihashi, F. W. van Ginkel, M. Noda, Y. Takeda, and J. R. McGhee. 1997. A nontoxic mutant of cholera toxin elicits Th2-type responses for enhanced mucosal immunity. *Proc. Natl. Acad. Sci. USA 94:5267.*
44. Di Fabio, S., I. N. Mbawuike, H. Kiyono, K. Fujihashi, R. B. Couch, and J. R. McGhee. 1994. Quantitation of human influenza virus-specific cytotoxic T lymphocytes: correlation of cytotoxicity and increased numbers of IFN-γ producing $CD8^+$ T cells. *Int. Immunol. 6:11.*
45. Yoshino, N., Y. Ami, K. Terao, F. Tashiro, and M. Honda. 2000. Upgrading of flow cytometric analysis for absolute counts, cytokines and other antigenic molecules of cynomolgus monkeys (*Macaca fascicularis*) by using anti-human cross-reactive antibodies. *Exp. Anim. 49:97.*
46. Honda, M., K. Matsuo, T. Nakasone, Y. Okamoto, H. Yoshizaki, K. Kitamura, W. Sugiura, K. Watanabe, Y. Fukushima, S. Haga, et al. 1995. Protective immune responses induced by secretion of a chimeric soluble protein from a recombinant *Mycobacterium bovis* bacillus Calmette-Guerin vector candidate vaccine for human immunodeficiency virus type 1 in small animals. *Proc. Natl. Acad. Sci. USA 92:10693.*
47. Gorny, M. K., A. J. Conley, S. Karwowska, A. Buchbinder, J. Y. Xu, E. A. Emini, S. Koenig, and S. Zolla-Pazner. 1992. Neutralization of diverse human immunodeficiency virus type 1 variants by an anti-V3 human monoclonal antibody. *J. Virol. 66:7538.*
48. Yamamoto, M., D. E. Briles, S. Yamamoto, M. Ohmura, H. Kiyono, and J. R. McGhee. 1998. A nontoxic adjuvant for mucosal immunity to pneumococcal surface protein A. *J. Immunol. 161:4115.*
49. Ohmura, M., M. Yamamoto, H. Kiyono, K. Fujihashi, Y. Takeda, and J. R. McGhee. 2001. Highly purified mutant E112K of cholera toxin elicits protective lung mucosal immunity to diphtheria toxin. *Vaccine 20:756.*
50. Miller, C. J. 1998. Localization of simian immunodeficiency virus-infected cells in the genital tract of male and female rhesus macaques. *J. Reprod. Immunol. 41:331.*
51. McGhee, J. R., J. Xu-Amano, C. J. Miller, R. J. Jackson, K. Fujihashi, H. F. Staats, and H. Kiyono. 1994. The common mucosal immune system: from basic principles to enteric vaccines with relevance for the female reproductive tract. *Reprod. Fertil. Dev. 6:369.*
52. McGhee, J. R., H. Kiyono, M. Kubota, S. Kawahata, C. J. Miller, T. Lehner, K. Imaoka, and K. Fujihashi. 1999. Mucosal Th1- versus Th2-type responses for antibody- or cell-mediated immunity to simian immunodeficiency virus in rhesus macaques. *J. Infect. Dis. 179:S480.*
53. Couch, R. B. 2004. Nasal vaccination, *Escherichia coli* enterotoxin, and Bell's palsy. *N. Engl. J. Med. 350:860.*
54. Mutsch, M., W. Zhou, P. Rhodes, M. Bopp, R. T. Chen, T. Linder, C. Spyr, and R. Steffen. 2004. Use of the inactivated intranasal influenza vaccine and the risk of Bell's palsy in Switzerland. *N. Engl. J. Med. 350:896.*

American Journal of Pathology, Vol. 165, No. 4, October 2004

Gastrointestinal, Hepatobiliary and Pancreatic Pathology

$CD4^+CD45RB^{Hi}$ Interleukin-4 Defective T Cells Elicit Antral Gastritis and Duodenitis

Taeko Dohi,*† Kohtaro Fujihashi,‡ Toshiya Koga,‡ Yuri Etani,‡ Naoto Yoshino,‡ Yuki I. Kawamura,* and Jerry R. McGhee†

From the Department of Gastroenterology, Research Institute, International Medical Center of Japan, Tokyo, Japan; the Departments of Oral Biology,‡ School of Dentistry, and The Immunobiology Vaccine Center, Department of Microbiology,† The University of Alabama at Birmingham, Birmingham, Alabama*

We have analyzed the gastrointestinal inflammation which develops following adoptive transfer of IL-4 gene knockout ($IL\text{-}4^{-/-}$) $CD4^+CD45RB^{Hi}$ (RB^{Hi}) T cells to severe combined immunodeficient (SCID) or to T cell-deficient, T cell receptor β and δ double knockout ($TCR^{-/-}$) mice. Transfer of $IL\text{-}4^{-/-}$ RB^{Hi} T cells induced a similar type of colitis to that seen in SCID or $TCR^{-/-}$ recipients of wild-type (wt) RB^{Hi} T cells as reported previously. Interestingly, transfer of both wt and $IL\text{-}4^{-/-}$ RB^{Hi} T cells to $TCR^{-/-}$ but not to SCID mice induced inflammation in the gastric mucosa. Notably, $TCR^{-/-}$ recipients of $IL\text{-}4^{-/-}$ RB^{Hi} T cells developed a more severe gastritis with erosion, apoptosis of the antral epithelium, and massive infiltration of macrophages. This gastritis was partially dependent on the indigenous microflora. Recipients of both wt and $IL\text{-}4^{-/-}$ RB^{Hi} T cells developed duodenitis with multinuclear giant cells, expansion of mucosal macrophages, and dendritic cells. Full B cell responses were reconstituted in $TCR^{-/-}$ recipients of RB^{Hi} T cells; however, anti-gastric autoantibodies were not detected. We have now developed and characterized a novel model of chronic gastroduodenitis in mice, which will help in our understanding of the mechanisms involved in chronic inflammation in the upper gastrointestinal tract of humans. ***(Am J Pathol 2004, 165:1257–1268)***

A number of murine models of colitis involve either aberrant T cell or cytokine expression. For example, spontaneous colitis develops in T cell receptor (TCR)-α gene knockout mice where aberrant T cells producing Th2-type cytokines actually mediate disease.[1–3] Perhaps the most useful murine model for both T cell and cytokine regulation of inflammatory bowel disease (IBD) has involved adoptive transfer of $CD45RB^{Hi}$ T cells from normal mice to either SCID[4–6] or to RAG 2 gene knockout ($RAG^{-/-}$) mice.[7,8] The transfer of RB^{Hi} T cells into SCID mice results in development of a severe mononuclear cell infiltration, epithelial cell hyperplasia, and tissue damage. Strong evidence has emerged provided that colitis results from enteric bacterial antigen (Ag)-driven Th1 cell induction,[9] since RB^{Hi} T cell transfer into SCID mice with reduced bacterial flora failed to develop large bowel disease.[10,11] Interestingly, T cell subsets producing TGF-β[12] and IL-10[13] in the RB^{low} T cell population, when co-delivered with RB^{Hi} T cells, actually suppressed colitis. The RB^{low} T cell population was enriched in $CD4^+CD25^+$ T regulatory (Tr) cells.[14] Despite this compelling evidence that RB^{Hi} T cells give rise to effector Th1 cells which mediate colitis, this model had not allowed study of either normal or abnormal B cell participation in the pathogenesis of $CD4^+$ T cells. Since the majority of antibody forming cells (AFCs) in humans and higher mammals reside in the gastrointestinal (GI) tract mucosa,[15,16] the impact of the presence of B cells and plasma cells in the mucosal pathology cannot be ignored. For example, we recently showed that dysregulated Th2 cells cause villus atrophy and goblet cell transformation in the small intestinal epithelium. Further, a wasting disease was seen and was mediated by excess IL-4 and the presence of B cells.[17]

Chronic GI tract inflammation is one of the most common types of inflammatory processes. For many years, gastric ulcers were thought to occur in susceptible individuals, especially those hypersecreting gastric hydrochloric acid.[18,19] However, it has become clear that gas-

Supported by U.S. Public Health Service National Institutes of Health Grants DK 44240, AI 18958, AI 43197, DE 12242, AI 35932, and DC 04976, and by grants and contracts from International Health Cooperation Research, the Ministry of Health, Labor, and Welfare, the Ministry of Education, Culture, Sports, Science, and Technology; the Japan Health Sciences Foundation and Organization; and The Organization for Pharmaceutical Safety and Research.

Accepted for publication June 21, 2004.

Address reprint requests to Taeko Dohi, M.D., Ph.D., Department of Gastroenterology, Research Institute, International Medical Center of Japan, 1-21-1 Toyama, Shinjuku-ku, Tokyo 162-8655, Japan. E-mail: dohi@ri.imcj.go.jp.

tritis, peptic ulcer disease, and gastric cancer are the result of infection with the bacterium *Helicobacter pylori*.[19,20] Gastritis has been reproduced in experimental animals gastrically infected with either *H. pylori* or related bacteria.[21-24] Thus, gastritis and duodenitis are directly related to *H. pylori* infection; however, surprisingly little is known about what causes chronic inflammatory responses in the upper GI tract. Although many groups have shown that disease severity is related to certain virulence factors associated with *H. pylori*, only a minority of individuals infected with virulent strains of *H. pylori* develop severe disease.[25] In animal models, IL-10-deficient mice infected with *H. pylori* exhibited enhanced gastritis, lower bacterial loads, and higher serum IgG antibody (Ab) titers when compared with control mice.[26] These results have suggested the importance of the host immune system in perpetuating the gastritis and duodenitis. Indeed, a gastritis model in mice with *H. pylori* infection showed that $CD4^+$ T cells were both necessary and sufficient for gastritis, and IFN-γ contributed to this inflammation.[27] Further, oral immunization of mice with the *H. pylori* urease induced protection against *H. pylori* infection, but was often associated with corpus gastritis, which is now recognized as post-immunization gastritis.[28-30] In addition, *H. pylori*-infected SCID mice reconstituted with splenic T cells from *H. pylori*-infected, C57BL/6 mice developed severe gastritis, however, host colonization of *H. pylori* did not correlate to the severity of gastritis.[31] Thus, cell-mediated immunity appears necessary for gastritis development, and does not necessarily relate to the bacterial load. Although still controversial, there is significant evidence that $CD4^+$ Th1-type responses contribute to *H. pylori*-induced gastritis in humans.[32] For example, IFN-γ and TNF-α are the major cytokines produced by gastric T cells from *H. pylori*-infected subjects.[33,34]

In the murine colitis models induced by adoptive transfer of RB^{Hi} T cells, the microflora is necessary for disease; however, no priming of donor T cells with pathogens was required.[10,11] Furthermore, no specific colitogenic bacterial species has been identified to date. Nonetheless, regulation of colitis by Tr cells seems to occur in both innate and adaptive immunity.[35] These results indicate that T cells from normal mice have the potential to induce inflammation in response to the indigenous bacteria; however, the healthy host simultaneously develops Tr cells that attenuate the disease producing T cells. Similar mechanisms for upper GI tract inflammation may be present; however, there have been no reports of a gastritis model in the absence of infection or deliberate immunization, except for autoimmune gastritis induced by neonatal thymectomy[36,37] or ionizing radiation.[38]

In this study, we hypothesized that normal T cells prepared from pathogen-free mice would contain a subset, which potentially could cause inflammation in the upper GI tract, as well as colitis. We describe a new type of RB^{Hi} T cell transfer model in $TCR^{-/-}$ mice that allows assessment of RB^{Hi} T cells in the presence of responsive B cells. We discovered that transfer of RB^{Hi} T cells from IL-4 gene knockout ($IL\text{-}4^{-/-}$) mice resulted in gastroduodenitis in the absence of infection by pathogenic bacteria. Our results suggest the $CD4^+$ Th1-type T cells mediate both colitis and gastroduodenitis in $TCR^{-/-}$ mice reconstituted with RB^{Hi} T cells.

Materials and Methods

Mice

Normal wild-type (wt), $IL\text{-}4^{-/-}$, IFN-γ gene knockout ($IFN\text{-}\gamma^{-/-}$) TCR β and δ chain-defective ($TCR^{-/-}$) and SCID mice on the C57BL/6 background were originally obtained from the Jackson Laboratory (Bar Harbor, ME). This mouse colony was maintained under pathogen-free conditions in flexible Trexler isolators at the University of Alabama at Birmingham (UAB) Immunobiology Vaccine Center Mouse Facility. A separate colony was also maintained in the Immunocompromised Mouse Facility of the Research Institute, International Medical Center of Japan (IMCJ, Tokyo, Japan). We periodically and extensively performed health surveillance on these colonies. These tests were performed in laboratories with expertise in laboratory animal health care (Jackson Laboratories, Charles River Laboratories, Wilmington, MA and Central Laboratories for Experimental Animals, Kawasaki, Japan). This analysis included serological testing for viral infections, bacterial cultures of the nasopharynx, stomach and cecum, ecto- and endoparasitic examinations, and histology of all major organs and tissues. Feces and the stomach were also tested for *Helicobacter spp.* in these laboratories, including *H. hepaticus, H. bilis, H. muridarum, and "H. rappini"*, by PCR.[39-42] No lesions or pathogens including *Helicobacter spp.* and intestinal parasites have ever been detected in these two separate mouse colonies. We obtained essentially identical results in the mouse facilities of both UAB and the IMCJ, and these experiments are quite reproducible. Although original reports indicated that $TCR^{-/-}$ mice develop intestinal inflammation,[3] they did not develop histologically obvious gastritis, duodenitis, or colitis in our mouse facility until they were 24 weeks of age, which is well beyond the time frame of our experiments.

Purification of T Cells

Splenic T cells for adoptive transfer were purified as described previously.[17] In brief, following lysis of erythrocytes, splenic T cells were enriched by passage through a nylon wool column, and then stained with phycoerythrin (PE)-conjugated anti-CD45RB (23G2), FITC-labeled anti-B220, anti-CD11b, and anti-CD8 monoclonal antibodies (mAbs) (BD PharMingen, San Diego, CA). The $CD45RB^{Hi}$ T cell subset was separated by flow cytometry using a FACS Vantage (Becton-Dickinson Co., Sunnyvale, CA). Sorted, $CD45RB^{Hi}$ subsets were > 99% pure by the reanalysis using anti-CD4 Ab, anti-TCR $\gamma\delta$ Ab, anti-NK1.1 Ab, and anti-Gr-1 Ab.

Adoptive Transfer of T Cells

In these studies, purified populations of RB^{Hi} T cells were adoptively transferred to 6- to 8-week-old $TCR^{-/-}$ mice. We routinely transferred 1.0×10^6 T cells by the intrave-

nous (i.v.) route. Body weight was monitored weekly, and mice were taken for analysis when their weight became less than 75% of the initial weight, or at 12 weeks after adoptive transfer of RB^{Hi} T cells.

Histological Analysis

The stomach was removed by excising the esophagus and the anal side of the gastro-duodenal junction, opened along the greater curvature, washed and extended. Next the stomach was cut longitudinally in the middle first, and a 3- to 4-mm-wide strip was prepared. The lateral side of this strip included the fundus, antrum, and gastro-duodenal junction. This side was cut for preparation of sections for histological examination. At least one such section from each mouse prepared in this manner was examined. Duodenal tissues were obtained from 0.5 cm to 3 cm from the gastro-duodenal junction. Colonic tissue was taken from the middle and distal parts of the large intestine. The tissues were opened, fixed in 5% glacial acetic acid in ethanol, and paraffin-embedded. Tissue sections (4 μm) were prepared and stained with hematoxylin and eosin (H&E). In some experiments, 6 μm-frozen sections were prepared, dried and fixed with cold acetone for 10 minutes, and subjected to histological analysis. The immunohistochemical staining was performed using FITC- or biotin-labeled anti-CD3, anti-CD4, anti-B220, anti-CD11b, and anti-CD11c mAbs, respectively (all from BD PharMingen, San Diego, CA), followed by FITC- or TRITC-labeled streptavidin (BD PharMingen). For the detection of IgA^+, IgG^+ or IgM^+ plasma cells, sections were reacted with biotin-labeled anti-mouse IgA Ab, TRITC-labeled anti-mouse IgG Ab and FITC-labeled anti-mouse IgM Ab (BD PharMingen) followed by aminocoumarin-labeled streptavidin. Apoptotic cells were detected by TdT-mediated dUTP nick end labeling (TUNEL) using the Apoptosis *in Situ* Detection Kit *Wako* (Wako Pure Chemicals Industries, Ltd., Osaka, Japan) on paraffin-embedded sections, according to the vender's protocol. To detect myeloperoxidase in granulocytes, sections were directly incubated with a substrate solution, 3,3′-diaminobenzidine tetrahydrochloride (Sigma Chemical Co., St. Louis, MO) in the presence of H_2O_2. Histological scores for gastritis were based on a summation of scores for cell infiltration (0, none; 1, moderate; 2, severe), epithelial hypertrophy (0, none; 1, moderate; or 2, severe), erosion (0, none; 1, focal; or 2, diffuse), giant cells (0, none; 1, less than 2; or 2, more than 3 per section), and deformity of pits (0, none; 1, moderate; or 2, severe). Histological scores for duodenitis and colitis were determined by severity of the inflammation (0, none; 1, mild; 2, moderate; or 3, severe). For histological examination, two observers performed all of the scoring. One was a pathologist who was not involved in this research, and for this examiner, the samples were provided in blinded fashion.

Purification of Lamina Propria Lymphocytes

Peyer's patches were excised from the intestinal wall, and small intestinal lamina propria lymphocytes (LPLs) were prepared as described previously.[43] Briefly, the intestinal tissue was treated with 1 mmol/L EDTA in phosphate-buffered saline (PBS) for 20 minutes to remove the epithelium. The tissue was then digested with type V collagenase (Sigma) for 20 minutes, and this step was repeated once more. The mononuclear cells were further purified by using a discontinuous Percoll gradient of 75% and 40%.

ELISPOT Assay

Enumeration of antibody forming cells (AFCs) was performed as described previously.[44] In brief, 96-well nitrocellulose plates (Millititer HA, Millipore, Bedford, MA) were coated with goat anti-mouse Ig (H+L) [Southern Biotechnology Associates (SBA), Birmingham, AL]. After blocking with 1% bovine serum albumin (BSA) in PBS, the LPLs were incubated for 4 hours at 37°C in moisturized atmosphere of 5% CO_2 in an incubator. After washing the plates, the captured Ig was visualized using peroxidase-labeled anti-mouse IgG, IgA or IgM (SBA). The spots in the individual wells were counted with the aid of a stereomicroscope.

Quantification of Plasma Immunoglobulin Levels

Plasma immunoglobulin (Ig) levels were determined by a sandwich ELISA using the combination of anti-mouse Ig (H+L) (SBA) and peroxidase-labeled anti-mouse IgG, IgA, or IgM (SBA) as described previously.[17]

RT-PCR for mRNA Analysis

Total RNA was prepared from gastric tissue or from separated cells using an RNA-Bee RNA isolation reagent (Tel-Test, Inc., Friendswood, TX). Complementary DNA was synthesized from RNA by reverse transcription (RT). The PCR primers for murine GAPDH used were 5′-AGCCAAACGGGTCATCATCTC and 5′-TGCCTGCTTCACCACCTTCTT; for TNF-α, 5′-TTCTGTCTACTGAACTTCGGGGTCATCGGTCC-3′ and 5′-GTATGAGATAGCAAATCGGCTGACGTGTGCC. The step-cycle program was set for denaturing at 95°C for 45 seconds, annealing at 60°C for 45 seconds, and extension at 72°C for 45 seconds for a total of 40 cycles. Expression of mRNA was assessed by quantitative PCR using a SYBR Green PCR Master Mix (Applied Biosystems, Warrington, United Kingdom) and ABI PRISM 7700 Sequence Detector (Applied Biosystems). Quantification of mRNA for IFN-γ and IL-10 was performed using ABI Taqman probes (Applied Biosystems). The PCR primers for IFN-γ were 5′-TGATCCTTTGGACCCTCTGA and 5′-GCAAAGCCAGATGCAGTGT, for IL-10, 5′-GCTCTTGACTACCAAAGCCAC and 5′-CATGCCAGTCAGTAAGAGCAGG. The Taqman probes used for IFN-γ were 5′-CCTCCTGCGGCCTAGCTCTGAGAC and for IL-10, AAGAGAGCTCCATCATGCCTGGCTCA. Threshold cycle numbers (C_T) were determined with Sequence Detector Software (version 1.7; Applied Biosystems) and transformed using the $\Delta C_T/\Delta\Delta C_T$ method as described by the manufacturer, with GAPDH used as the calibrator gene.

Quantification of Cytokine Production and Intracellular Cytokine Analysis

For quantification of cytokines, $CD4^+$ T cells were purified from freshly prepared LPLs by staining with FITC-labeled anti-CD4 mAb (BD PharMingen) followed by flow cytometry with a FACS Vantage system. The purified $CD4^+$ T cells were added to wells of plates coated with anti-CD3 mAb (10 μg/ml, clone 145–2C11; BD PharMingen) and cultured in RPMI 1640 supplemented with 10% fetal calf serum (FCS), sodium pyruvate, L-glutamine, HEPES, and 50 μmol/L 2-mercaptoethanol (complete medium). Cultures were incubated for 48 hours at 37°C in 5% CO_2 in a moist air incubator. Cells in culture were removed, separated by centrifugation, and the supernatants were then subjected to a cytokine-specific ELISA, as described previously.[43] Briefly, microtiter plates were coated with mAbs to individual cytokines and blocked with 3% BSA in PBS at 37°C for 2 hours, and then diluted samples were added to well and incubated overnight at 4°C. Captured cytokines were detected using biotinylated detection mAbs and peroxidase-labeled anti-biotin mAb (Vector Laboratories Inc., Burlingame, CA). The following mAbs were used for coating and detection, respectively: anti-IFN-γ, R4–6A2 and XMG 1.2; anti-IL-2, JES6–1A12 and JES6–5H4 mAbs; anti-IL-4, BVD4-1D11 and BVD6–23G2. For intracellular cytokine analysis, LPLs were cultured in plates coated with anti-CD3 mAb in complete medium with anti-CD28 mAb. After 48 hours of culture, the cells were subjected to intracellular cytokine staining as described previously.[45] In brief, cells were stained with FITC-labeled anti-CD4 mAb (BD PharMingen), fixed, permealized, and then stained with PE-labeled anti-IFN-γ mAb (BD PharMingen) for analysis using flow cytometry.

Treatment with Antibiotics and Bacterial Culture

In some experiments, recipient mice were given a combination of antibiotics in their drinking water. Metronidazole (0.6 g/L, Wako Pure Chemical Industries Ltd.), neomycin (0.35 g/L, Wako), streptomycin (0.2 g/L, Wako), and bacitracin (0.35 g/L, Wako) were added to the drinking water, and the mice were continuously given this water *ad libitum* until the histological and cytological analyses were performed. To determine total colony forming units (CFU), mice were treated with antibiotics as above for 6 weeks, fasted for 6 hours and then the entire stomach was removed, washed three times with PBS, minced and homogenized with 2 ml of PBS in a Teflon-glass homogenizer. This homogenate was then subjected to serial dilution and spread over culture plates. Anaerobic bacteria were cultured on GAM agar plates (Nissui Pharmaceuticals, Tokyo, Japan) in culture jars (GasPack System BBL, Becton Dickinson) with AneroPac (Mitsubishi Gas Chemical Co, Inc., Tokyo, Japan). For aerobic cultures, brain-heart infusion agar (Difco, Becton Dickinson), chocolate agar, and sheep blood agar plates (both from Nissui) were used. To examine for the presence of indigenous microflora in the oral cavity, the mucosal surfaces of oral cavity were swabbed, and the swabs were placed in 300 μl of PBS. Then 100 μl of this suspension was spread over a culture plate. Anaerobic cultures were initiated within 20 minutes after taking samples. After 24 hours of incubation at 37°C, numbers of CFU were enumerated.

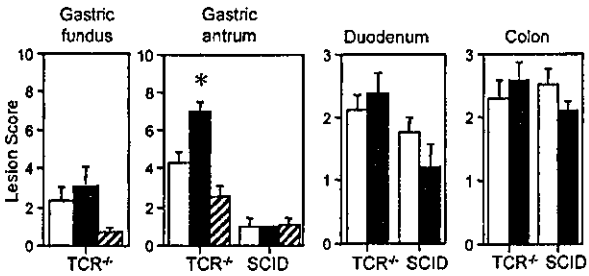

Figure 1. Histological scores of gastritis, duodenitis and colitis. $TCR^{-/-}$ or SCID mouse recipients were given RB^{Hi} T cells prepared from splenocytes of wt (**blank column**, $n = 8$), IL-$4^{-/-}$ (**solid column**, $n = 10$) or IFN-$\gamma^{-/-}$ (**hatched column**, $n = 7$) mice. The results shown are the mean and SEM. *, Difference between wt and IFN-$\gamma^{-/-}$ mice was statistically significant.

Statistics

The results were compared by the Mann-Whitney test using the Statview II statistical program (Abacus Concepts, Berkeley, CA) adapted for Macintosh computers. The results were considered to be statistically significant if P values were less than 0.05.

Results

Inflammation of the GI Tract in $TCR^{-/-}$ and SCID Mouse Recipients

Previous studies have shown that the transfer of RB^{Hi} T cells resulted in severe colitis in either SCID or $RAG^{-/-}$ mouse recipients, and the colitis was mediated by $CD4^+$ Th1-type cells.[4–6,9,46] A similar type of colitis was induced in $TCR^{-/-}$ recipients of wt RB^{Hi} T cells. Recipients of IL-$4^{-/-}$ RB^{Hi} T cells also developed a severe colitis (Figure 1). We noted that $TCR^{-/-}$ recipients of either wt or IL-$4^{-/-}$ RB^{Hi} T cells developed a duodenitis with a heavy cell infiltration, which was rarely described in SCID recipients previously. These changes were limited to the duodenum within 5 cm of the pylorus, and both the jejunum and ileum remained normal. We also found that these mouse recipients developed an inflammation of the stomach, especially in the antral region. When recipients of wt, IL-$4^{-/-}$, or IFN-$\gamma^{-/-}$ RB^{Hi} T cells were compared, recipients of IL-$4^{-/-}$ T cells developed the most severe gastritis and those mice receiving IFN-$\gamma^{-/-}$ T cells showed only minimal changes (Figure 1). Interestingly, SCID recipients of either wt or IL-$4^{-/-}$ RB^{Hi} T cells showed mild lesions in the stomach, with only slight cell infiltration. Adoptive transfer of wt or IL-$4^{-/-}$ $CD45RB^{low}$ T cells did not result in gastritis, duodenitis, or colitis (data not shown).

Pathological Features of Gastritis

In all 10 $TCR^{-/-}$ recipients of IL-$4^{-/-}$ RB^{Hi} T cells, the gastric antral and duodenal mucosa were increased in

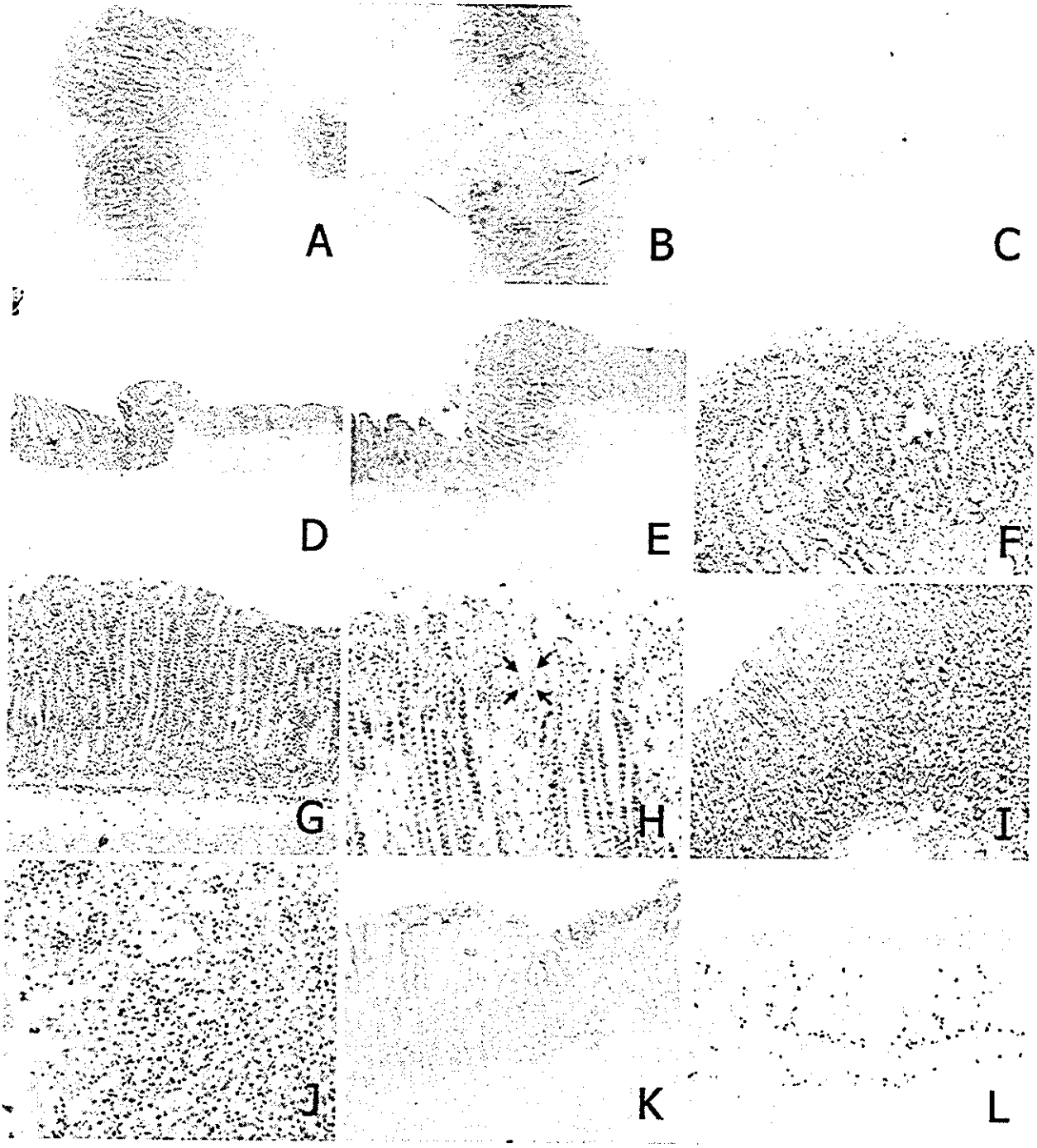

Figure 2. Macroscopic and histological features of murine gastritis. **A:** Normal stomach tissue taken from naïve $TCR^{-/-}$ mice. **B:** Inflamed stomach from $TCR^{-/-}$ mice after adoptive transfer of $IL\text{-}4^{-/-}$ RB^{Hi} T cells. **C:** The gastroduodenal junction of naïve $TCR^{-/-}$ mice. **D:** The gastroduodenal junction of the SCID recipients given $IL\text{-}4^{-/-}$ RB^{Hi} T cells. **E:** The gastroduodenal junction of the $TCR^{-/-}$ recipients given $IL\text{-}4^{-/-}$ RB^{Hi} T cells. **F:** The inflamed gastroduodenal junction with erosion. **G** and **H:** Antral gastritis with surface erosion and elongation of pits of $TCR^{-/-}$ recipients of $IL\text{-}4^{-/-}$ RB^{Hi} T cells. **Arrows** indicate a multinuclear giant cell. **I:** The fundic lesion with mild changes was taken from the same specimen as shown in **G**. **J:** Cell infiltration and dilated pits including migrating cells in the surface of the gastric fundic region in $TCR^{-/-}$ recipients of $IL\text{-}4^{-/-}$ RB^{Hi} T cells. **K:** Histochemistry for peroxidase of the antral region $TCR^{-/-}$ recipients of $IL\text{-}4^{-/-}$ RB^{Hi} T cells. As positive control, a section from a mouse with colitis induced by dextran sulfate with neutrophil infiltration was used (**L**). Sections were counterstained with methylgreen. Images were captured using a ×4 objective lens (**C**, **D** and **E**), ×20 lens (**G**, **I**, **K**, and **L**) or ×40 lens (**F**, **H**, and **J**).

thickness and exhibited an overall turbid appearance. In five recipients of $IL\text{-}4^{-/-}$ RB^{Hi} T cells, the gastric fundic area was also edematous, and erosions with petechiae were seen (Figure 2, A and B). Histological examination revealed that the inflammation was accompanied by hypertrophy of glands and elongation of pits, and these changes were most evident at the gastro-duodenal junction (Figure 2, C to F). Most typically, the antral glands were elongated more than twofold longer than their normal length with pit dilatation in some parts, and mononuclear cell infiltration in the

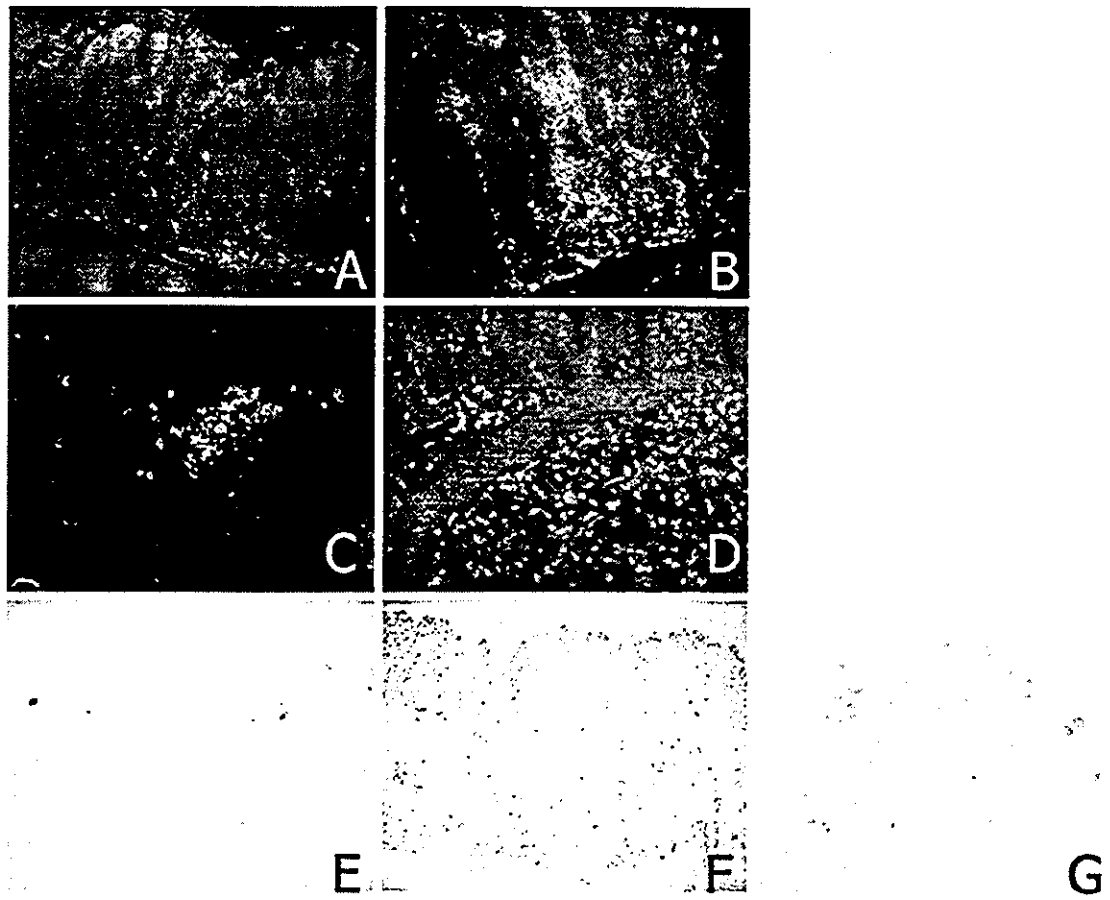

Figure 3. Immunohistochemistry and detection of apoptosis. $CD4^+$ T cells in the antrum of a SCID recipient of IL-$4^{-/-}$ RB^{Hi} T cells (**A**). $CD4^+$ T cells (**B**), $B220^+$ cells (**C**), and $CD11b^+$ cells (**D**) in the inflamed antrum of $TCR^{-/-}$ mouse recipients of IL-$4^{-/-}$ RB^{Hi} T cells. Apoptotic cells were detected by TUNEL in $TCR^{-/-}$ recipients of wt RB^{Hi} T cells (**E**) or IL-$4^{-/-}$ RB^{Hi} T cells (**F** and **G**). Images were captured using a ×20 objective lens (**A-F**) or ×100 lens (**G**).

recipients of wt and IL-$4^{-/-}$ RB^{Hi} T cells was seen (Figure 2G). In addition to these findings, recipients of IL-$4^{-/-}$ RB^{Hi} T cells developed surface erosions with multinuclear giant cell infiltration (Figure 2H). Neutrophil infiltration was not frequent in the stomach or the duodenum as shown in the histochemical reaction of myeloperoxidase (Figure 2, K and L). In 50% of IL-$4^{-/-}$ T cell recipients, a fundic inflammation with mononuclear cell infiltration and deformity of glandular pits with cells migrating into the dilated pits were seen (Figure 2J), while the other 50% of mice showed only mild changes (Figure 2I). In both cases, destruction specific for parietal cells was not seen. In the inflamed stomach, a massive infiltration of $CD4^+$ T cells occurred (Figure 3B), an event scarcely seen in SCID recipients (Figure 3A). Furthermore, B cell aggregates were also detected by staining with anti-B220 mAb (Figure 3C). We also assessed the presence of plasma cells in the inflamed areas; however, no IgG-, IgA- or IgM-containing cells were seen in the gastric mucosa by immunostaining (data not shown). The infiltrating cells were mostly macrophage-like cells as shown by staining with anti-CD11b Ab (Figure 3D). On the other hand, there was no expansion of $CD11c^+$ dendritic cells in the inflamed stomach (data not shown). Since surface erosion was enhanced in the gastric mucosa of recipients of IL-$4^{-/-}$ RB^{Hi} T cells, we also assessed apoptosis. In recipients of wt RB^{Hi} T cells, although there was elongation of glands and a cell infiltration, apoptotic cells were rare in the epithelium (Figure 3E). In contrast, in recipients of IL-$4^{-/-}$ RB^{Hi} T cells, the numbers of apoptotic cells were clearly increased. Apoptosis was readily detected in the infiltrating cells in all layers of the mucosa and especially in the surface epithelium (Figure 3, F and G).

Pathological Features of Duodenitis

Duodenal inflammation was seen in $TCR^{-/-}$ mouse recipients of both wt and IL-$4^{-/-}$ RB^{Hi} T cells. The villi and crypts were both remarkably elongated, and the villi were dilated due to the cell infiltration (Figure 4, B and C). In the lamina propria, multinuclear giant cells were frequently seen; however, granulomas were absent (Figure 4D). Immunohistological analysis revealed an infiltration of $CD4^+$ cells (Figure 4E), expansion of dendritic cells and an infiltration of macrophages (Figure 4F), which were not seen in naive $TCR^{-/-}$ mice.

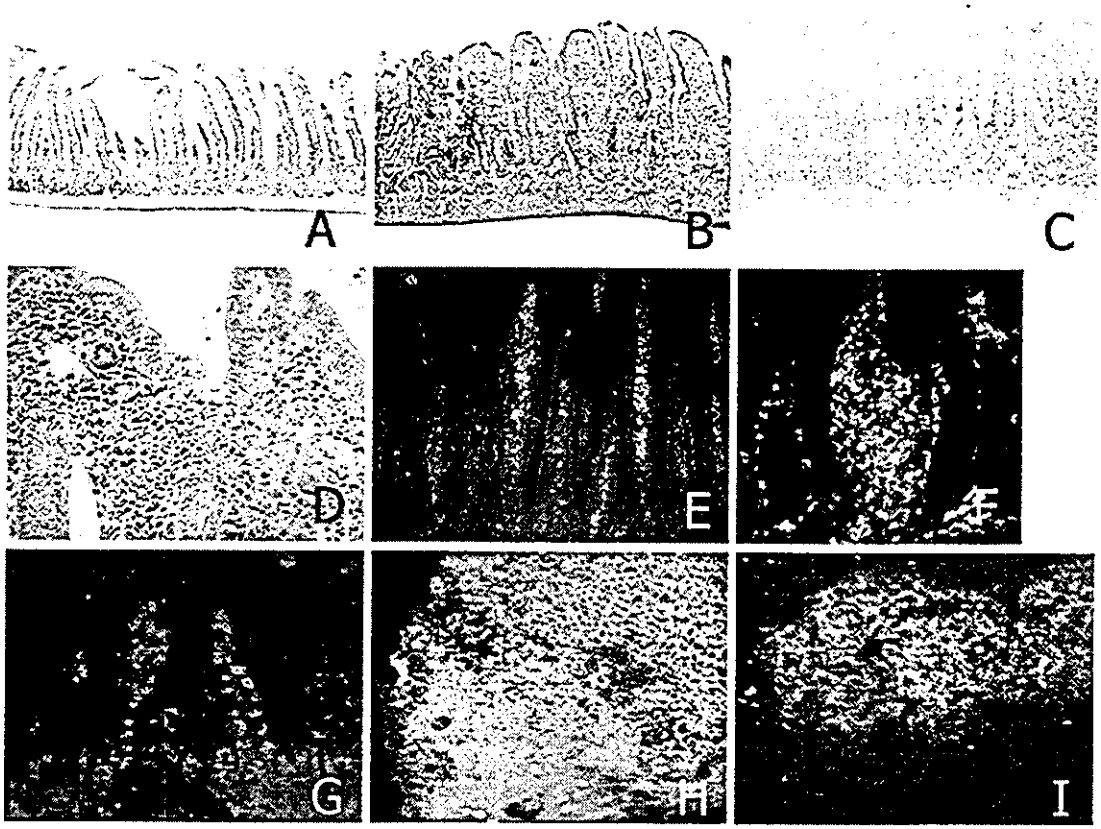

Figure 4. Histological features of murine duodenitis. **A:** H&E staining of duodenum of $TCR^{-/-}$ mice without cell transfer. **B:** Inflamed duodenum of $TCR^{-/-}$ recipients of wt RB^{Hi} T cells. **C** and **D:** Inflamed duodenum of $TCR^{-/-}$ recipients of IL-$4^{-/-}$ RB^{Hi} T cells. Dilated villus of duodenal tissue was stained with anti-CD4 (green, **E**), and anti-CD11b (green) and anti-CD11c (red) mAbs (**F**). Some $CD11c^{+}$ cells also express CD11b. **G:** IgA AFCs in the duodenum of recipients of wt RB^{Hi} T cells. **H:** Peyer's patches from recipients of wt RB^{Hi} T cells stained with anti-B220 (green) and anti-CD3 (red) mAbs. **I:** Peyer's patches of $TCR^{-/-}$ mice without T cell transfer. Images were captured using a ×10 objective lens (**A-C**), ×20 (**E**), or ×40 lens (**D**, **F–I**)

Production of Cytokines

To assess cytokine production by T cells that infiltrated the mucosa of adoptive hosts, $CD4^{+}$ T cells were isolated from LPLs of the small intestine. The $CD4^{+}$ T cells recovered from recipients of wt or IL-$4^{-/-}$ RB^{Hi} T cells released both IFN-γ and IL-2 (Figure 5A). It should be noted that T cells from the recipients of wt RB^{Hi} T cells also produced high levels of IL-4 (Figure 5A). We also noted that T cells infiltrating the gastric mucosa produced IFN-γ in the $TCR^{-/-}$ recipients of IL-$4^{-/-}$ T cells (Figure 5B), although T cells from recipients of IL-$4^{-/-}$ T cells tended to contain slightly more IFN-γ producing cells than recipients of wt RB^{Hi} T cells, as determined by flow cytometry (Figure 5B). Thus, IFN-γ release by T cells recovered from recipients of wt or IL-$4^{-/-}$ RB^{Hi} T cells were, for the most part, comparable. However, the lack of IL-4 secretion resulted in a remarkable phenotype, which contributed to the distinct and severe gastritis in $TCR^{-/-}$ recipients of IL-$4^{-/-}$ RB^{Hi} T cells. Further, to prove that the milder gastritis in SCID than in $TCR^{-/-}$ recipients of IL-$4^{-/-}$ RB^{Hi} T cells, we quantitatively assessed TNF-α, IFN-γ, and IL-10 by RT-PCR from total RNA extracts taken from the gastric antrum. Expression of IFN-γ and TNF-α in $TCR^{-/-}$ recipients was higher than those seen in SCID recipients (Figure 5C).

Mucosal and Systemic B Cell Responses in $TCR^{-/-}$ Recipients of RB^{Hi} T Cells

It should be noted that $TCR^{-/-}$ recipients of either wt or IL-$4^{-/-}$ RB^{Hi} T cells exhibited IgA-positive cells in the small intestine, including the duodenum (Figure 4G). Peyer's patches were also reconstituted with distinct T and B cell zones (Figure 3H), which were filled with $B220^{+}$ cells in $TCR^{-/-}$ mice before T cell transfer (Figure 3I). The plasma Ig levels were also elevated following adoptive transfer of either wt or IL-$4^{-/-}$ RB^{Hi} T cells. The IgG levels were comparable in both groups; however, the IgA levels were lower in recipients of IL-$4^{-/-}$ RB^{Hi} T cells than recipients of wt RB^{Hi} T cells (Figure 6A). The numbers of AFCs in the small intestine in $TCR^{-/-}$ recipients were also reconstituted by adoptive transfer of RB^{Hi} T cells. Numbers of IgG and IgA secreting cells were much less frequent in $TCR^{-/-}$ recipients of IL-$4^{-/-}$ T cells than those mice given wt T cells (Figure 6B). Thus, systemic IgG responses were fully reconstituted in both groups of mice; however, recipients of IL-$4^{-/-}$ T cells exhibited little class switching to the IgG or IgA isotypes. Plasma from these mice did not contain autoreactive Abs when assessed by the binding capacity to sections prepared from the stomach of naïve mice.

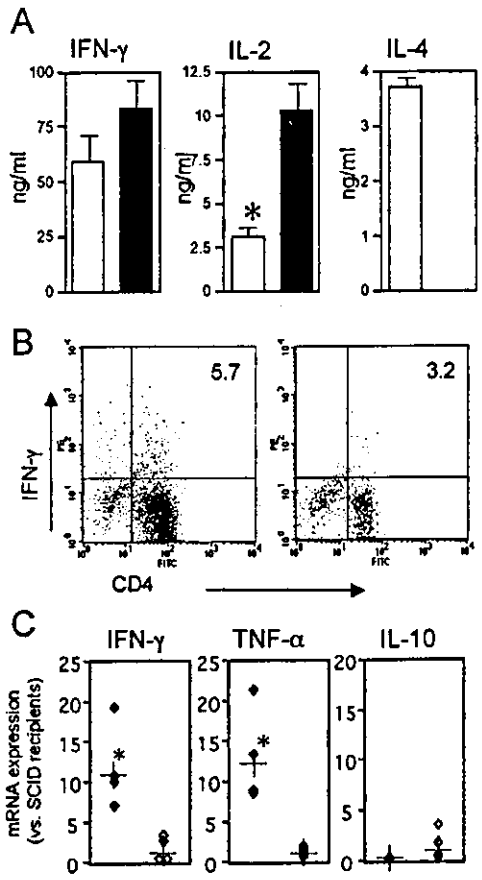

Figure 5. Production of cytokines by CD4$^+$ T cells infiltrating the GI tract. **A:** CD4$^+$ T cells were isolated from the small intestine of TCR$^{-/-}$ recipients of wt (**blank column**) or IL-4$^{-/-}$ (**solid column**) RB^{Hi} T cells and stimulated with anti-CD3 mAb for 48 hours. Culture supernatants were subjected to a cytokine ELISA. Values shown are the mean of three experiments obtained from pooled cells from three mice in each group. The results shown are the mean and SD. The difference was statistically significant. **B:** Production of IFN-γ by infiltrating cells. LPLs were prepared from the inflamed gastric mucosa of TCR$^{-/-}$ recipients of IL-4$^{-/-}$ (**left**) or wt (**right**) RB^{Hi} T cells, stimulated with anti-CD3 and anti-CD28 mAbs for 48 hours, and subjected to intracellular cytokine analysis. **C:** Relative expression of mRNA for cytokines in the stomach in TCR$^{-/-}$ and SCID recipients of IL-4$^{-/-}$ RB^{Hi} T cells determined by quantitative RT-PCR. Total RNA was extracted from the antral mucosa, and mRNA for individual cytokines and GAPDH were analyzed. Based on the average ΔC_T value of four SCID recipients, data from individual mice were shown as relative expression to SCID mice. Results from four mice are shown and the results indicated as (+) are the average of relative expression for each group. *, Statistically significant difference from SCID recipients.

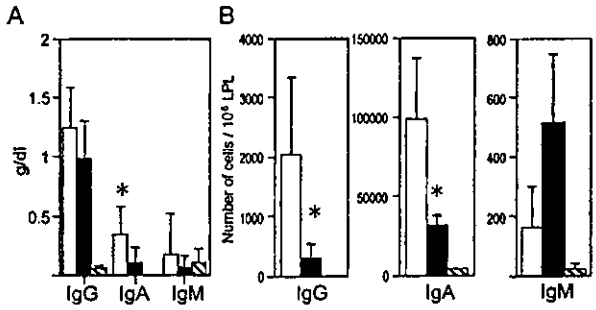

Figure 6. Reconstitution of systemic and mucosal Ig production. **A:** Plasma Ig levels in TCR$^{-/-}$ recipients of wt RB^{Hi} T cells (**blank column**), IL-4$^{-/-}$ RB^{Hi} T cells (**solid column**) or naïve TCR$^{-/-}$ mice (**shaded column**). **B:** Numbers of IgG, IgA, or IgM secreting cells in the small intestinal LPLs isolated from TCR$^{-/-}$ recipients of wt (**blank column**), IL-4$^{-/-}$ RB^{Hi} (**solid column**) or naïve TCR$^{-/-}$ mice (**hatched column**) was determined by ELISPOT assay. Values shown are the mean and a SD of each group containing 4 to 7 mice.

Gastritis Was Dependent on the Presence of a Microflora

To this point, we found that gastritis was induced in the TCR$^{-/-}$ recipients of RB^{Hi} T cells without infection of pathogenic bacterial strains. However, the indigenous microflora in the upper GI tract or bacteria in ingested food may play a role in the induction of gastritis. To clarify this, we gave mice neomycin, streptomycin, bacitracin, and metronidazole in their drinking water following transfer of IL4$^{-/-}$ RB^{Hi} T cells. This treatment essentially eliminated the indigenous flora in the oral cavity and the stomach (Table 1), and efficiently suppressed the gastritis. Interestingly, the effect on gastritis was efficient but only partial, whereas colitis was completely blocked in these mice (Figure 7). These results indicated that induction of gastritis was partially dependent on the indigenous microflora, while colitis essentially required its presence.

Discussion

We have established a new model for gastritis that is induced by adoptive transfer of RB^{Hi} T cells incapable of production of IL-4 (Th1-prone T cells). The gastritis and duodenitis develops in the absence of a particular bacterial pathogen, such as *Helicobacter spp.* and is also distinct from autoimmune models of gastritis. The first major finding was that this pathogen-free gastritis developed after adoptive transfer of IL-4$^{-/-}$ RB^{Hi} T cells into TCR$^{-/-}$ mice. Gastritis did not occur after transfer of IL-4$^{-/-}$ RB^{Hi} T cells into SCID mice, clearly suggesting a requirement for B cell responses for full-blown gastric inflammation. Finally, adoptive transfer of IL-4$^{-/-}$ RB^{Hi} T cells yielded greater mucosal damage when compared with TCR$^{-/-}$ recipients of wt RB^{Hi} T cells. Each of these significant new findings is discussed in more detail below.

Numerous studies have attempted to establish *in vivo* models for gastric inflammation following infection with *H. pylori*. In our model, we successfully induced gastritis without bacterial infection or specific immunization. Of course, several models for autoimmune gastritis are induced in the absence of pathogens. Autoimmune disease induced by thymectomy[36,37] or ionizing radiation[38] have both resulted in gastritis. These types of gastritis were associated with damage of parietal cells or loss of parietal and chief cells by autoantibodies to the gastric H$^+$/K$^+$-ATPase.[47,48] A similar type of autoimmune gastritis occurs spontaneously in C3H/He mice.[49] "Autoimmune gastritis" and "colitis induced in SCID/Rag2$^{-/-}$ recipients of RB^{Hi} T cell transfer" are both caused by the absence of CD4$^+$CD25$^+$ regulatory T cells, because gastritis was induced in nu/nu mice recipients of CD25$^-$ T cells prepared from CD25$^+$ cell-depleted mice.[50] However, these two models have not been compared with each other very often. Importantly, autoimmune gastritis